HHS Public Access
Author manuscript
J Neurosci Res. Author manuscript; available in PMC 2019 January 01.

Published in final edited form as:
J Neurosci Res. 2018 July ; 96(7): 1223–1242. doi:10.1002/jnr.24225.

Polyethylene glycol solutions rapidly restore and maintain axonal continuity, neuromuscular structures and behaviors lost after sciatic nerve transections in female rats

Michelle Mikesh[1], **Cameron L. Ghergherehchi**[2], **Robert Louis Hastings**[1], **Amir Ali**[1], **Sina Rahesh**[1], **Karthik Jagannath**[1], **Dale R. Sengelaub**[3], **Richard C. Trevino**[4], **David M. Jackson**[5], and **George D. Bittner**[1]

[1]Department of Neuroscience, University of Texas at Austin, Austin, Texas 78712, USA

[2]Institute for Cellular and Molecular Biology, University of Texas at Austin, Austin, Texas 78712, USA

[3]Department of Psychological and Brain Sciences, Indiana University, Bloomington, Indiana 47405, USA

[4]Department of Orthopedic Surgery, Wellspan Teaching Hospitals, York, PA, USA

[5]Neuraptive Therapeutics, Lafayette CO, USA

Abstract

Complete severance of major peripheral mixed sensory-motor nerve proximally in a mammalian limb produces immediate loss of action potential conduction and voluntary behaviors mediated by the severed distal axonal segments. These severed distal segments undergo Wallerian degeneration within days. Denervated muscles atrophy within weeks. Slowly-regenerating (~1mm/d) outgrowths from surviving proximal stumps that often non-specifically reinnervate denervated targets produce poor, if any, restoration of lost voluntary behaviors. In contrast, in this study using completely transected female rat sciatic axons as a model system, we provide extensive morphometric, immunohistochemical, electrophysiological, and behavioral data to show that these adverse outcomes are avoided by microsuturing closely apposed axonal cut ends (neurorrhaphy) and applying a sequence of well specified solutions, one of which contains polyethylene glycol (PEG). This “PEG-fusion” procedure within minutes re-establishes axoplasmic and axolemmal continuity and signaling by non-specifically fusing (connecting) closely apposed open ends of severed motor and/or sensory axons at the lesion site. These PEG-fused axons continue to conduct action potentials, generate muscle action potentials and muscle twitches for months and do not

Corresponding Author: George D. Bittner, Department of Neuroscience, The University of Texas at Austin, 2415 Speedway, Austin, TX 78712, Phone: 512-923-3735, Fax: 512-471-9651, bittner@austin.utexas.edu.
Associate Editor: J. Regino Perez-Polo

Author Contributions

All authors had full access to all the data in the study and take responsibility for the integrity of the data and accuracy of the data analysis. *Conceptualization*, MM, CLG, RLH,RCT,GDB; *Methodology*, MM, CLG, RLH, RCT, DRS, DMJ, GDB; *Investigation*, MM, CLG, RLH, AA, SR, KJ; *Formal Analysis*, MM, CLG, RCT, DRS, DMJ, GDB; *Writing*, MM, CLG, RLH, AA, SR, KJ, RCT, DRS, DMJ, GDB; *Supervision*, MM, CLG, RCT, DRS, DMJ, GDB; *Funding Acquisition*, RCT, DRS, DMJ, GDB.

Conflict of Interest Statement

The authors declare no conflicts of interest.

undergo Wallerian degeneration. Continuously-innervated muscle fibers undergo much less atrophy compared to denervated muscle fibers. Dramatic behavioral recovery to near-unoperated levels occurs within days to weeks, almost certainly by activating many CNS and PNS synaptic and other plasticities, some perhaps to a greater extent than most neuroscientists would expect. Negative Control transections in which neurorrhaphy and all solutions except the PEG-containing solution are applied produce none of these remarkably fortuitous outcomes observed for PEG-fusion.

Graphical abstract

Soleus neuromuscular junctions 7 days after a complete sciatic transection with PEG-fusion (PEG) or gold standard microsuture repair (-PEG). PEG-fusion repair maintains nerves (arrow) and neuromuscular functions, and restores near-normal voluntary behaviors within weeks.

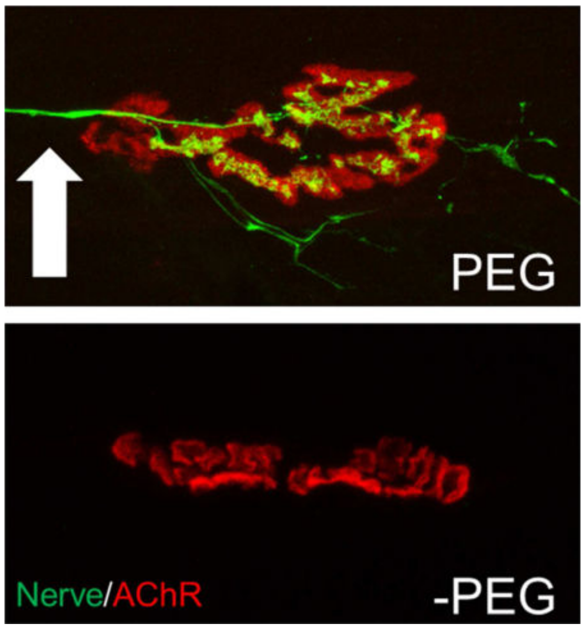

Keywords

axotomy; polyethylene glycol; Wallerian degeneration; nerve repair; nerve regeneration; sciatic nerve

Introduction

Peripheral nerve injuries (PNIs) that involve a transection, ablation, or severe crush are the most common nerve-involved traumatic injuries in civilian and military populations and significantly burden health care systems (Allan, 2000; Stansbury et al., 2007; Cross et al., 2011). Such PNIs interrupt axonal continuity, thereby immediately producing complete loss of sensory and motor functions of denervated structures followed by obligatory Wallerian degeneration of the distal axonal segments within several days (Bozkurt et al., 2008; Campbell, 2008; Burch, 2011; Brushart, 2011; Kandel et al., 2013). For a single transection in the clinic or in experimental laboratory models, the current "gold standard" treatment is to closely appose the severed proximal and distal ends of the nerve with microsutures ("neurorrhaphy") to encourage surviving axons proximal to the lesion to slowly (~1mm/day) regenerate. These regenerating axons often imperfectly reinnervate distal targets after many months, or even years, in rats or larger mammals. PNIs repaired by neurorrhaphy often have poor outcomes in the clinic and experimental animal models in part due to (**1**) regeneration inaccuracy; and (**2**) atrophy of target muscles after long periods of denervation before re-innervation might occur (Campbell, 2008; Brushart, 2011; Green and Wolfe, 2011; Kandel et al., 2013).

We have previously reported an axonal repair technique that consists of a series of pharmaceutical agents in solution, one of which contains the membrane fusogen polyethylene glycol (PEG), in conjunction with neurorrhaphy of singly-transected nerves (Bittner et al., 2012, 2016a,b, 2017a,b; Ghergherehchi et al., 2016). This PEG-fusion technique produces dramatic improvements in the speed and quality of behavioral (functional) recovery as measured by the Sciatic Functional Index (SFI) in a rat sciatic nerve model system. These papers present extensive evidence that PEG-fusion produces: (**1**) Immediate (within minutes) restoration of axolemmal and axoplasmic continuity of many axons because **a**) compound action potentials (CAPs) conduct, and **b**) intracellular dyes passively diffuse across the lesion site; (**2**) dramatically better, more rapid, and permanent recovery of sciatic-mediated behaviors compared to Negative Control animals receiving neurorrhaphy at 7–42 postoperative (PO) days.

However, neither we nor any other author (Bamba et al., 2016a; 2017; Riley et al., 2017) has extensively examined the morphological and functional basis for these results, i.e., the structure and/or function of severed distal axons, neuromuscular junctions (NMJs) and muscle fibers in PEG-fused versus Unoperated or Negative Control sciatic nerves at 0d–42d PO. We have also never directly examined whether or how behavioral recovery at various PO days is due to (**1**) immediate reinnervation by axons that are artificially PEG-fused and then continuously maintained *and/or* (**2**) delayed reinnervation by natural regeneration of axons proximal to the lesion site.

In this study at 0d–42d PO using transmission electron microscopy (TEM) and or immunohistochemical staining (IHC), we have extensively examined the microanatomy of axons, myelin, neuromuscular junctions (NMJs), and muscle fibers distal to a complete transection of female rat sciatic nerves in the mid-thigh repaired by neurorrhaphy with and without using our PEG-fusion technique. We have also examined the function of severed distal axons and NMJs as assessed by their ability to conduct extracellularly-recorded action potentials (compound action potentials: CAPs) across the transection site that evoke extracellularly recorded muscle action potentials (CMAPs) and muscle twitches. We also examine functional/behavioral recovery by assessing locomotor ability as assessed by the Sciatic Functional Index (SFI). Finally, we examine how these various measures correlate with each other and especially with the SFI, given that behavioral recovery is by far the most important measure of regenerative success, perhaps the only truly relevant measure (Brushart, 2011; Bittner et al., 2012, 2016a,b, 2017a,b; Riley et al., 2015; Ghergherehchi et al., 2016; Mikesh et al., 2017).

We confirm that PEG-fusion immediately (within minutes) restores axolemmal and axoplasmic continuity of many axons across the lesion site. As previously reported, we also confirm that behavioral recovery often approaches levels seen in Unoperated animals by 42d PO. We extensively document that PEG-fused myelinated axons and their NMJs survive for at least 42d PO, i.e., PEG-fusion prevents Wallerian degeneration. None of these results are observed in Negative Control animals. *Most importantly, highly significant behavioral recovery is routinely observed to occur within 21d PO in PEG-fused animals at a time when no target tissues have been reinnervated by myelinated axons regenerating by outgrowth.*

After a single transection given the above results, we conclude that PEG-fused myelinated axons, NMJs and the muscles they innervate are completely responsible for the dramatically improved speed and quality of behavioral recovery compared to Negative Control animals at 21d PO and largely responsible for the extensive behavioral recovery at 42d PO. Although an examination of the specificity of CNS or PNS connections is beyond the scope of this paper, these results are obtained even though non-specific connections may be made either by axons “artificially” PEG-fused or by axons “naturally” regenerating by outgrowth. Finally, all these results suggest that adoption of a PEG-fusion technology for acute repair of transection PNIs could produce a paradigm shift from current clinical practice.

Methods

Surgery

All experimental procedures were approved by, and performed in accordance with the standards set forth by, the Institutional Animal Care and Use Committee at the University of Texas at Austin. Animals were maintained on a 12hr:12hr reverse light:dark cycle and given food and water ad libitum. Surgical and behavioral procedures were performed during the active cycle for these animals. For complete surgical details, please refer to Ghergherehchi et al. (2016). We have used both male and female rats in previous papers, and shown that PEG-fusion results for both sexes are very similar for CAP restoration, dye diffusion, muscle fiber morphology, and SFI recovery (Britt et al., 2010; Bittner et al., 2012, 2016a,b; 2017a,b; Riley et al., 2015; Sexton et al., 2012; Rodriguez-Feo et al., 2013; Ghergherehchi et al., 2016). We used females in this study because we examined effects of PEG-fusion on these same structures. Examining both sexes could nearly double animal use because statistical analyses in our previous papers showed that a group size of (n) = of 4–6 each at 2–6 time points provided statistical power to detect differences of $p \leq 0.05$ of $\geq 20\%$ between an experimental and a control group. Our results at UT Austin have shown good reproducibility when replicated by investigators at Vanderbilt in papers cited above.

Briefly, 53 female Sprague-Dawley rats weighing 225–300g were anesthetized with a small mammal isoflurane inhaled anesthetic system (Handlebar Anesthesia, Austin, TX). After initial induction using a 4% isoflurane/oxygen mixture at a flow rate of 1.5 liters/min, animals were then maintained with a 1.5–2% mixture at 1 liter/min for the duration of the surgery. The lateral aspect of the left hindlimb was trimmed of fur and disinfected with 10% iodine/povidone. A 2–3 cm incision was made through the skin and the biceps femoris, parallel to its muscle fibers; muscle fibers were then separated to expose the sciatic nerve. The sciatic nerve was completely transected in the animal’s extracellular fluid with fine surgical scissors under sterile conditions. The nerve was then flushed with sterile Plasmalyte A (Baxter, Deerfield, lL), a calcium-free hypotonic saline, to open cut ends and expel many intracellular vesicles that form to seal cut axonal ends. The severed and opened nerve ends were carefully trimmed and treated with an antioxidant (1% methylene blue, MB; Acros Organics, Morris Plains, NJ) in sterile distilled water to keep axonal ends open and prevent formation of additional intracellular vesicles (Lore et al., 1999; Britt et al., 2010; Spaeth et al., 2010, 2012; Bittner et al., 2012, 2016). The proximal and distal nerve segments were closely apposed with microsutures that provide mechanical strength at the lesion sites to prevent PEG-fused axons from pulling apart because axonal (or other cell-type) plasmalemmas have minimal tensile strength (Bittner et al., 2012, 2016a,b; 2017a,b; Ghergherehchi et al., 2016).

Animals were randomly assigned to PEG-fused or Negative Control groups after the neurorrhaphy was performed to eliminate bias in surgical procedure. In PEG-fused animals, after neurorrhaphy, a sterile hypotonic solution of 50% w/w polyethylene glycol (Sigma Aldrich, St. Louis, MO 3.35 kDa) in distilled water was applied to the repair site for 1–2 minutes to non-specifically repair/join/fuse closely apposed open cut axonal ends. This solution was omitted for Negative Control animals. The microsutured ends of both PEG-fused and Negative Control nerves were then irrigated several times with sterile isotonic Lactated Ringers containing calcium to repair axolemmal holes with calcium-induced vesicles (Krause et al., 1994; Spaeth et al., 2010, 2012). The incision wound was closed with sutures and the animal was allowed to recover on heated pads.

Electrophysiological analyses—Compound action potentials (CAPs) are evoked action potentials extracellularly recorded from a set of nerve axons. We regard CAPs as only a “yes/no” (binary) measure of PEG-fusion success because CAP amplitude and time course depend on so many variables, including electrode shape, construction and placement, and numbers of axons having different diameters and myelin wrappings (Ghergherehchi et al., 2016). CAPs were evoked to assess electrophysiological function and continuity (Lore et al., 1999; Riley et al., 2015). Stimulating and recording electrodes were placed ~1cm apart across the site of intended transection and a CAP was recorded to confirm that the sciatic was intact and electrically viable. Continuity of axoplasm and axolemma across the lesion site after PEG-fusion was confirmed by demonstrating that CAPs were conducted across the coaptation site after PEG-fusion repair.

Compound muscle action potentials (CMAPs) are evoked action potentials extracellularly recorded from a set of muscle fibers. Due to a set of uncontrolled variables, including electrode placement and muscle fiber properties, CMAPs are also only a binary measure of PEG-fusion success. CMAPs were evoked by stimulating the sciatic nerve in the upper thigh and recording from the tibialis anterior muscle. The stimulating electrode was placed proximally to any coaptation site, and a pair of monopolar needle electrodes were placed in either the tibialis anterior muscle. Care was taken during the recording to limit stimulus current delivered to the sciatic nerve to avoid direct ephaptic activation of these muscles. Stimulation of the transected sciatic nerve may sometimes evoke CMAPs or twitches in distal muscle masses by collateral branches that sometimes arise proximal to the proximal stimulating electrodes (Rupp et al., 2007). These CMAPs are no longer observed if the collateral branch is subsequently also transected.

Behavioral analyses

The Sciatic Function Index (SFI) is a common and reliable test to assess function and return of behaviors mediated by the sciatic nerve in rats and mice (de Medinaceli et al., 1982; Wood et al., 2011). The SFI score is highly dependent upon foot flexion and toe spread, movements controlled by lower leg and foot muscles innervated by the sciatic nerve, e.g., tibialis anterior, soleus, or gastrocnemius muscles. Unoperated or Sham Control animals have SFI scores ranging from −20 to +20; Negative Control animals typically have SFI scores ranging from −120 to −80. Any recovery is typically associated with gradual decreases in the absolute value of negative SFI scores as axons regenerating by outgrowth from severed surviving proximal axonal stumps that increasingly re-innervate more denervated distal muscle fibers.

Animals were handled for acclimation and trained in the testing procedure for at least one week prior to surgery. For SFI tests run by testers blinded to their experimental group, both hind paws were marked with red or blue ink, right side unoperated and left injured, respectively. The rat was placed upon an inclined 100mm wide board, 5 feet in length, lined with paper strips. After the rat ran back to its home cage across the paper-lined board, the paper was collected for measuring footprints by testers blinded to treatment. Runs without stops or hesitation producing three consecutive footprints of the left and right foot were scored and recorded. Two successful runs were collected for each rat per testing day (Britt et al., 2010; Ghergherehchi et al., 2016). For both the normal and the experimental sides, assessors blinded to their treatment measured six variables for the normal and experimental footprints: footprint length, total toe spread, and intermediate toe spread as previously reported (Carlton and Goldberg, 1986). The average of the six values for both the experimental and normal side from the two runs was recorded as the SFI score for the day. Animals were first tested 3d after surgery, then weekly for at least 42d PO. Data was recorded in spreadsheets and graphs were prepared in Graphpad Prism 7. PEG-fused animals were deemed to have a successful recovery if they achieved an SFI score of -59 or better by 42d PO, a value 3SD greater than obtained by Negative Control animals at 42d PO (Ghergherehchi et al., 2016); significant recovery at $p < 0.05$ would be an SFI score of − 75 or better in this and previous studies.

Immunohistochemical analyses

After euthanasia, soleus muscles were taken from Unoperated rats and the operated sides of PEG-fused (n=6) or Negative Control (n=4) rats 7, 10, or 21d PO. To label intramuscular nerves and NMJs, muscles were dissected into Phosphate Buffered Saline pH 7.4 (PBS, Fisher Scientific) and pinned into Sylgard coated dishes prior to fixation and permeabilization in −20°C methanol, then rehydrated and washed in PBS (Kang et al., 2007). Muscles were placed in microcentrifuge tubes and blocked with 0.2% BSA, 0.3% TritonX-100 in PBS with 0.1% Azide for 30 minutes. SV2 (anti-synaptic vesicle protein 2, Developmental Studies Hybridoma Bank) and 2H3 (anti-neurofilament, DSHB) were added (1:400 each in blocking solution) and the muscles maintained overnight at 4°C. Muscles were then washed in blocking solution and incubated in anti-mouse Alexa 488 (1:600, Molecular Probes, Invitrogen) for one hour at room temperature. Bungarotoxin conjugated to Alexa 647 (1:800, Molecular Probes, Invitrogen) was used to label the acetylcholine receptors prior to washes in PBS. Thin sheets of muscle fibers were dissected from the muscle surface and mounted on glass slides with Permafluor (Thermo Scientific).

Morphological analyses of sciatic axons and nerves

After a rat was euthanized by cardiac KCl or Euthasol, sciatic nerves were removed from Unoperated animals (n=3) or from experimental animals (n=23) at 7, 10, 14, 21, or 42D PO. The nerves were placed into 0.1M sodium cacodylate buffer followed by 2% paraformaldehyde/3% glutaraldehyde fixative in buffer, or rats were perfused transcardially with buffer followed by fixative. Sciatic nerves and soleus muscles were pinned into Sylgard dishes with fixative overnight at room temperature. The next day, tissues were washed with buffer, trimmed and post-fixed in 1% osmium tetroxide/1% potassium ferrocyanide in 0.1M sodium cacodylate buffer for 3–5 hours, washed in water, stained in 1% aqueous uranyl acetate for 1–2h, and then washed and held in water (Smith et al., 2013). Segments of Unoperated nerve used to compare to distal operated nerve segments were sampled in the distal third of the nerve, not including the peroneal-tibial bifurcation. Specifically, proximal and distal nerve segments were sampled 4–6 mm proximal and distal to the transection, respectively. Much care was taken to ensure that sampling sites were equivalent in all nerves relative to suture placement.

Tissues were dehydrated though graded alcohols, exchanged to absolute acetone, placed in increasing concentrations of Hard Plus Resin 812 (Electron Microscopy Sciences, Hatfield, PA) and then embedded in fresh resin and polymerized at 60° C. Glass knife thick sections (0.5μm) were stained in toluidine blue and examined for orientation and regions of interest with light microscopy prior to trimming for thin sectioning. Thin sections (silver-gold, 65nm) were cut on a diamond knife (DDK, Wilmington, DE) and mounted on formvar-coated Synaptek grids (Electron Microscopy Sciences, Hatfield, PA) prior to viewing in a Technai Spirit electron microscope (Hillsboro, OR) fitted with an AMT Advantage HR 1kX1k digital camera. Neuromuscular junctions, muscles and multiple regions within and around sciatic nerves were imaged for further analyses.

For axonal morphometrics, we followed the methodology described by Michailov et al., (2004) and Sherman et al. (2012). Nerve composition was adapted from similar methods developed by these authors in other publications and used here to describe the occupation of space in the nerve overall (Smith, 2013). For proportional area composition data, images totaling ≥10,000 μm^2 were selected at random; images including major section folds or large capillaries were excluded. All myelinated axon, myelin, and degrading debris profiles were traced and measured in ImageJ (Schneider et al., 2012). Extracellular space, small capillaries, and other cell types were categorized as interspace (de Medinaceli, 1995). The percent composition was calculated for each profile type as a proportion of the total measured area.

For axon morphology, 10–20 electron micrographs per nerve were taken at 1700x. To avoid bias, all intact *en face* axons in an image were measured until at least 100–150 were recorded, except for some Negative Controls for which <100 axons could be counted in many images. Individual axons were excluded if they exhibited redundant or separated myelin layers, myelin infolds that crossed the axon midline, or electron-dense axoplasm. Traces of axons, nerve fibers, and debris were measured in ImageJ and recorded. Axon diameter was calculated as (√axon area/π)*2, fiber diameter was calculated as (√fiber area/π)*2, and g ratio was calculated as axon diameter/fiber diameter.

Analyses of NMJs and muscle fibers

Muscles (n=21) were prepared either for resin embedding and area measurement or immunohistochemical labeling and innervation assessment. For muscle fiber area, animals were perfused with fixative prior to overnight fixation. After embedding, thick plastic sections (0.5μm) from NMJ regions where the nerve inserts at the belly of soleus muscles were imaged. At least 100 muscle fibers for each muscle were traced in ImageJ and the measurements recorded. For synaptic ultrastructure, thin sections (approximately 65nm) were cut from regions with NMJs and imaged with TEM at 8 – 43kx.

To assess soleus muscle innervation, NMJs were observed with a Zeiss Axiovert 200M (Pleasanton, CA) by first locating bungarotoxin labeled acetylcholine receptors (AChRs) with a CY5/647 filter and then switching to an Alexa 488 filter to detect innervation by labeled nerve axons. Labeled axons parfocal and in contact with a receptor were considered to innervate the receptor. Confocal images were captured on a Zeiss LSM 710 with a 40× oil immersion lens and compressed z-stacks of images prepared in ImageJ.

Statistical analyses

Excel was used to calculate means, linear regressions and t-test comparisons. For axons, Welch's t-tests, a test that allows for heteroscedastic data, n = the number of animals in a treatment group, N = the total number of axons in a treatment group, and N-2 = the degrees of freedom. Cohen's *d* effect size was calculated as the difference between two means divided by a standard deviation for the data (Cohen, 1998; Sawilowsky, 2009). A two-tailed Student's t-test, a test for homoscedastic data, was used to compare mean SFI scores for each treatment group on a given post-operative day. Two-way ANOVAs were used to analyze means and standard errors of SFI scores (Bittner et al., 2012; Riley et al., 2015; Ghergherehchi et al., 2016; Mikesh et al., 2018).

The distribution of nerve axon diameters in an undamaged nerve is bimodal, and thus is not a normal distribution. In analyzing axon diameters in Negative Control animals, left shifts in distribution are always observed. We used t-tests because they are the standard test of axon or nerve fiber diameter in peripheral nerve models when comparing conditions or treatments (Ikeda et al., 2012; Cragg and Thomas 1964; Sherman et al., 2012).

Results

Terminology

We use the terms "**reinnervation**", "**regeneration**", and "**PEG-fusion**" according to their generally accepted meanings. These and other terms are explicitly defined below because their inappropriate use (Robinson and Madison, 2017) can/has led to incorrect understandings of the mechanism of action of PEG-fusion, how to test its results, and unwarranted conclusions about negative clinical benefits. **Reinnervation** is the restoration of a nerve supply to a denervated structure by any means at any time after denervation**. Regeneration** is slow (1–2mm/day) axonal outgrowth from severed proximal nerve segments that may or may not ever successfully innervate a denervated structure. **PEG-fusion** is the rapid (within minutes) reconnection/repair of many (but not all) axons in severed proximal and distal axonal segments by a defined protocol involving sequential administration of pharmaceutical agents in solution, one of which contains the membrane fusogen PEG (Lentz, 2007), to induce ***immediate*** reinnervation of some otherwise denervated target tissues (Bittner et al., 2012, 2016a,b; 2017a,b; Ghergherehchi et al., 2016). PEG-fusion does not prevent axons that are not PEG-fused from extending outgrowths from surviving proximal stumps. Thus, reinnervation after PEG-fusion may, and likely does, occur through two mechanisms: immediate axonal reconnection by (artificial) PEG-fusion and/or by delayed spontaneous innate nerve regeneration by natural, slower, axonal outgrowth. Both regeneration and PEG-fusion can produce specific or non-specific reinnervation of a structure by its original axons**. Nerve axon** refers to the axoplasm and axolemma but does not include its glial sheath; **nerve fiber** refers to the axon and its glial sheath. *In this study, we examine only myelinated nerve axons and myelinated nerve fibers.* A **peripheral nerve** (e.g., sciatic nerve) refers to its nerve fibers and connective tissue sheaths (endoneurium, perineurium, and epineurium) that contain various structures and cell types (connective tissue, blood vessels, Schwann cells, fibroblasts, macrophages, etc.).

Electrophysiological evidence that PEG-fusion produces and maintains axonal continuity and reduces or prevents Wallerian degeneration: CAPs and CMAPS

As described above in Methods and previous publications (Bittner et al., 2012, 2016a,b; 2017a,b; Ghergherehchi et al., 2016), we always confirmed that CAPs are conducted from proximal to distal in intact sciatic nerves before lesioning, entirely eliminated after lesioning and restored within minutes after PEG-fusing the transection site of a singly-cut sciatic nerve (Fig. 1a; Unop, PEG) - or at any PO time a rat was sacrificed from 7d (Fig. 1b: PEG) to 42d PO (Fig. 1c) to more than 100d PO (Bittner et al., 2012, 2016a,b;2017a,b). These CAP recordings demonstrate that at least some sciatic nerve axons maintain morphological and functional continuity across the lesion site from 0 - >100d PO in PEG-fused sciatic nerves. In contrast, as previously reported (Bittner et al., 2012, 2016a,b; 2017a,b; Ghergherehchi et al., 2016), CAPs did not conduct across the transection site immediately after transection or for up to at least 7d PO if the microsutured nerve was not PEG-fused (Fig. 1a,b; NC). At 42d PO, a small CAP with a slower conduction velocity was often detected in Negative Control sciatic nerves, almost-certainly due to regenerating small-diameter axons.

CMAP recordings taken from the tibialis anterior after sciatic nerve stimulation showed proximal-to-distal conduction in intact sciatic nerves (Fig. 1d; Unop). After transection and suture repair of the sciatic nerve, CMAPs almost always could not be recorded when the sciatic nerve was stimulated proximal to the lesion site (Fig. 1d; NC), unless the nerve was PEG-fused (Fig. 1d; PEG). CMAPs were also recorded at 7d–42d PO in PEG-fused rats

(Fig. 1e,f; PEG), but not in rats for which the nerve was not PEG-fused at 7d PO (Fig. 1e; NC). At 42d PO (Fig. 1f) or later, a relatively small CMAP with a longer stimulus-response latency could sometimes be recorded in Negative Control rats, presumably because some smaller-diameter, less well-myelinated, motor axons regenerating by outgrowth from the proximal stump had reinnervated and activated muscle fibers. [Smaller diameter, less well-myelinated, motor axons conduct CAPs more slowly than larger diameter, better myelinated fibers thereby producing longer-latency CMAPs.] These CMAP data show that PEG-fused axons are not only able to conduct and maintain electrophysiological signals across a lesion site within minutes after PEG-fusion, but also that NMJ function is immediately restored and maintained by PEG-fusion.

CMAPs were sometimes generated by ephaptic current spread or aberrant proximal sciatic motor branches and were not as reliable a measure of axonal continuity across a lesion site as CAPs (Rupp et al., 2007). Ephaptic activation of CAPs has not been observed in this or previous studies (Britt et al., 2010; Bittner et al., 2012, 2016a,b;2017a,b; Riley et al., 2015; Ghergherehchi et al., 2016).

CAPs and CMAPs recorded distal to the transection site were associated with twitches of muscles innervated by axons distal to the lesion site in PEG-fused nerves at all PO times, indicating that NMJs were functional from 0d to at least 42d PO. CAPs and CMAPs recorded distal to the transection site were associated with twitches of muscles innervated by axons distal to the lesion site in Negative Control nerves only at 42d PO or later, indicating that functional NMJs were not present from 0d to at least 21d PO, and then some functional NMJs were present at 42d PO.

Behavioral evidence that PEG-fusion produces and maintains axonal continuity and reduces or prevents Wallerian degeneration: SFI scores

As described in Methods and in previous publications (Bittner et al., 2012, 2016a,b Bittner et al., 2017a,b; Ghergherehchi et al., 2016), the Sciatic Functional Index (SFI) is a sensitive test for voluntary behavioral control of the lower limb. Unoperated animals in this study had SFI scores ranging from −15 to +3 (Table 2, Fig. 2), values within the range seen in previous studies (Bittner et al., 2012, 2016a,b; 2017a,b; Brushart, 2011). We tested the SFI of PEG-fused, and Negative Control animals at 3, 7, 14, 21, 35 and 42d PO in this study (Fig. 2a–b) and also at weekly intervals thereafter in previous studies (Fig. 2c, historical data). Negative Control animals had SFI scores ranging from −69 to −120 for all PO times and −94 to −74 at 42d PO, also within the range seen in previous studies cited above. That is, most (10/11) Negative Control animals exhibited no significant recovery at 7d–42d PO (Table 2, Fig. 2). One Negative Control animal (E36 in Table 2) showed significant ($p<0.05$) recovery to an SFI score of −74. Compared to Negative Control SFI scores at 42d PO, all PEG-fused animals had an SFI score better than −75 or −59 that represent significant behavioral recovery at $p < 0.05$ and $p < 0.01$, respectively (see Methods). In PEG-fused animals, significant behavioral recovery to an SFI core of −75 was usually (7/10) *not* observed before 14d PO, but usually was observed (5/7) by 21d PO. [Note that animals sacrificed for morphological analyses at earlier PO times are not part of the SFI sample at later PO times.]

Significant functional (behavioral) recovery always occurred for PEG-fused nerves (5/5) sampled at 42d PO.

Figure 2c shows the average SFI scores for animals used in the current study (colored lines), as well as our historical data from animals generated using the same surgical protocols (black lines). There was no significant difference ($p > 0.05$) between our historical data and the current data produced for either Negative Control or PEG-fused animals and values for significant behavioral recovery were unchanged (see Methods). PEG-fused animals recovered significantly compared to Negative Control animals by 14d PO, ($p = 0.028$ Student's t-test). Behavioral recovery for PEG-fused animals was also significantly higher compared to Negative Controls at 21d PO ($p = 0.009$), 28d PO ($p = 0.0003$), 35d PO ($p = 0.0004$), and 42d PO ($p = 0.0012$).

Consistent with the SFI score that assesses overall function of the sciatic nerve, representative footprints (Fig. 2d) showed recovery of PEG-fused animals compared to Negative Controls within 42d PO. Unoperated, but not Negative Control, animals were able to lift their heel and spread their toes during normal gait (Fig. 2d). PEG-fused animals regained the ability to spread toes and lift their heel almost completely within 42d PO and walked with a near-normal gait. In contrast, Negative Control animals rarely gained an ability to spread their toes and often dragged their heels during locomotor gait for the entire testing period. Individual SFI scores of animals tested for 42d PO (Fig. 2a,b) showed that PEG-fused animals had unequal amounts of recovery, i.e., some animals recovered to near baseline, while others recovered significantly, but not completely. This variation is likely due to variation in the number of sciatic axons that were successfully PEG-fused. Negative Control animals exhibited much less variation in SFI scores from 3d–42d PO (Fig. 2a–c), in large part because they all showed little or no recovery of behavioral function compared to successfully PEG-fused nerves.

Morphological evidence that PEG-fusion produces and maintains axonal continuity and reduces or prevents Wallerian degeneration: gross structure of sciatic nerves

The gross anatomical features of Unoperated and 0d – 42d PO PEG-fused and Negative Control sciatic nerves (Fig. 3) were examined using a dissecting microscope. Figure 3a,b shows that intact, unoperated sciatic nerves in the mid-thigh of rats are usually about 1mm in diameter, glisten white, and can vary in fascicle arrangement in different animals (or even in the same animal). Branching patterns can affect the ability to align and suture distal and proximal cut ends that retract 1–2 mm after transection. PEG-fused (Fig. 3c) and Negative Control (Fig. 3d) nerves at 0d PO appeared similar to intact, Unoperated nerves, with some residual methylene blue staining at the coaptation site. At 42d PO, PEG-fused distal segments withstood mild stretching and retained the white color of intact nerves (Fig. 3e), often with mild inflammation around the suture site. In contrast, Negative Control nerves at 42d PO had lost their white glistening appearance (Fig. 3f). These Negative Control distal segments were very fragile and did not withstand mild stretching.

Morphological evidence that PEG-fusion produces and maintains axonal continuity and reduces or prevents Wallerian degeneration: TEM

Type of data shown in Figs 4–7 and Tables 2–3—Tissue level features and more detailed axon morphology were examined with TEM at 1.7 - 6kx (Figs. 4–7), NMJs at 8 – 20kx, and filamentous ultrastructure and myelin layers of individual axons at 26 – 43kx at 80kv (Fig. 8). Figure 4 shows representative electron micrographs of transverse-sectioned Unoperated sciatic nerves (far left column) and sciatic nerves receiving PEG-fusion (top row) or Negative Control (bottom row) repair protocols from unoperated and severed nerves 4–6 millimeters distal to the transection site at 7, 21, and 42d PO. Figure 5 shows higher power TEM of viable and degenerated axons. Figure 6 shows histograms of the diameter distribution of (myelinated) *nerve fibers* for PEG-fused and Negative Control sciatic nerves at 7–14, 21, and 42d PO compared to Unoperated severed sciatic nerves. Figure 7 shows box plots of the range and average diameters of (myelinated) *nerve fibers* for their 1st–4th quartile and the median value of their total distribution. The average ± SD (or SEM for SFIs) for axon and fiber diameters, etc., for these and other figures are given in Table 2. Statistical comparisons are given in Table 3.

Morphology of Unoperated myelinated axons and nerve fibers—Unoperated myelinated nerve fibers (Fig. 4a,e; Fig. 5a) had the ultrastructural appearance of viable axons described in many previous studies (see Brushart, 2011) such as electron lucid axoplasm containing mitochondria (Fig.5a: arrowhead) and filaments (neurofilament, tubulin) in lengthwise orientation within the axon. Each myelinated axon was surrounded by rings of electron dense myelin. Unoperated axons averaged 3.82±1.64µm in diameter and had a 0.61±0.06 g ratio. Unoperated nerve fibers had average diameters of 6.2µm. The average of the ten largest nerve fibers (MAX_{10}) was 11.6µm (Table 2). Figures 6 and 7 show that Unoperated fibers range from 1–15µm in a bimodal distribution similar to that reported in other studies (Gutmann and Sanders, 1943; Berthold et al., 1983; Fields and Ellisman, 1986; Brushart, 2011; Ikeda and Oka, 2012).

The proximal segments of PEG-fused or Negative Control nerves underwent relatively few changes compared to Unoperated nerves (Figs. 4–8) at 7d – 42d PO. In contrast, distal segments of Negative Control nerves underwent more drastic morphological changes at 7d – 42d PO compared to PEG-fused nerves (Figs. 4–7, Table 2).

Morphology of PEG-fused vs. Negative Control myelinated axons and fibers at 7–14d PO—The morphology of PEG-fused and Negative Control myelinated axons was consistent for each protocol at the three different specific PO sampling times and could be combined. At all three times, many PEG-fused axons had the ultrastructural appearance of viable intact unoperated axons described above. At 7–14d PO, many PEG-fused nerve axons were present, myelinated, and displayed features characteristic of intact axons (Figs. 4–7 and Table 2). However, the average diameters of nerve axons and nerve fibers (2.7 and 4.2µm, respectively) were smaller than Unoperated axons and fibers (3.8 and 6.2µm, respectively). However, the largest 10 myelinated nerve fibers in each sample (MAX_{10} in Table 2) averaged 13.5µm were larger than Unoperated fibers (11.9µm). At 7–14d PO, PEG-fused axons had higher g ratios (0.66) compared to Unoperated axons (0.61). Nerve axon and fiber diameters were near normal in an animal whose SFI scores showed significant recovery at 10d PO. In contrast, Negative Control nerves (Fig. 4f–h, bottom row) consistently had **no** intact myelinated axons at any time 7–14d PO and had the ultrastructural appearance of axons that had undergone Wallerian degeneration: That is, at 7d PO, myelin sheaths of some axons were still identifiable, but axoplasm was highly disorganized (Fig. 5c). By 14d PO, myelin sheaths were collapsed or enlarged and debris was reduced (Fig. 4f–h). Hence, nerve axon diameter, nerve fiber diameter and myelin thickness were consistently assigned a value of 0μm in Figures 6–7 and Table 2 at all three PO times. PEG-fused axonal diameters had a bimodal distribution.

Morphology of PEG-fused vs. Negative Control axons and fibers at 21d PO— PEG-fused sciatic nerves 6–7mm distal to transection sites (Fig. 4b–d, top row) had axons and myelin sheaths that appeared relatively normal at 21d PO as did the range of axon and nerve fiber diameters. At 21d PO, Negative Control axons 4–6mm distal to the transection site were uniformly small with normal-appearing axoplasm and normal, albeit thin, myelin sheaths (Fig. 4). That is, Negative Control axons had an average diameter of 1.72±0.44μm and an average g ratio of 0.76±0.05, with a clear single peak of axonal diameters, ranging from 1-6μm, consistent with findings in other studies on regenerating peripheral nerves (Gutmann and Sanders, 1943; Fields and Ellisman, 1986; Wolthers et al., 2005; Brushart, 2011; Ikeda and Oka, 2012). The average and range of nerve axon and nerve fiber diameters for Negative Control nerves (Figs. 6–7, Table 2) were consistently smaller than values for PEG-fused nerves and the variation among Negative Control nerves was smaller and similar to axons regenerating by outgrowth reported by others cited above.

Morphology of PEG-fused vs. Negative Control axons and fibers at 42d PO— PEG-fused sciatic nerves 6-7mm distal to transection sites (Fig. 4d, top row) continued to have axons and myelin sheaths that appeared normal with average diameters slightly smaller and myelin sheaths slightly thinner than Unoperated axons and fibers, i.e., PEG-fused axons had an average diameter of 2.77±1.25μm and a 0.70±0.08 g ratio. The distribution and MAX_{10} of PEG-fused nerve fiber diameters were similar to values found for Unoperated nerves.

At 42d PO the axoplasm of viable axons in Negative Control nerves was similar to that in Unoperated axons, but Negative Control average axonal diameters were smaller (1.90±0.83μm) and their average g ratios were higher (0.65±0.09). Nerve fibers in Negative Control nerves averaged 3.0 and 3.2μm with MAX_{10}=4.8 and 6.7μm, respectively. At 42d PO, Negative Control sciatic nerve fibers distal to a microsutured transection had significantly smaller diameters than PEG-fused fibers and a much smaller range, consistent with axons regenerating by outgrowths from surviving proximal stumps reported in other studies (Gutmann and Sanders, 1943; Fields and Ellisman, 1986; Wolthers et al., 2005; Brushart, 2011; Ikeda and Oka, 2012; see Discussion). PEG-fused axonal diameters had a bimodal distribution.

Summary of differences—Table 3 shows the outcomes of comparisons between Unoperated, PEG, and Negative Control axons at 7–14, 21, and 42d PO. Since there are no myelinated axons in 7–14d PO Negative Control nerves, comparisons at this PO time are only between PEG and Unoperated groups. Though Negative Control axons gain thicker myelin from 21 to 42d PO, there is little change in average axon diameter as noted in Table 3. Unoperated, PEG-fused, and Negative Control nerves are significantly different at all PO times ($p < 0.001$); PEG-fused axonal or fiber diameters are significantly larger than Negative Control values ($d > 0.8$) at 21d and 42d PO. Though Cohen's *d* changes from 2.62 to 0.44 when comparing Negative Control to Unoperated axons with respect to g ratio, there is little change in *d* (1.75– 1.48) for axons during the same time. These results and differences listed numerically in Table 2 are shown graphically in Figures 5 and 6.

Morphological evidence that PEG-fusion produces axon continuity and reduces or prevents Wallerian degeneration: nerve composition

Figure 8 shows the composition by PO time and treatment type per 10,000μm^2 of Unoperated nerves taken in mid-thigh versus PEG-fused and Negative Control nerves taken 4– 6mm distal to single transection sites as observed in lower-power TEM images similar to those shown in Figures 4 and 5. Myelin and axon areas were measured separately: axon area was defined as electron lucid, intact, normally structured interiors to electron dense myelin rings. Debris areas were defined as osmophilic structures not seen in intact nerve such as dissociated myelin, condensed axon material, or material engulfed within macrophages. Interspace areas were defined as electron lucid open space or normally observed non-neuronal cells (e.g., Schwann cell bodies, fibroblasts) and structures (e.g., small capillaries, perineurium). Interspace area was calculated as the total area minus the sum of axon, myelin, and debris areas. Each type of area was converted to the percent of 10,000μm^2 that it occupied.

Unoperated nerves (n=3) were composed of 27±1% axonal area (average ± SD), 47±3% myelin, 0±0.5% debris, and 26±3% interspace with 191±18 axons per 10,000μm^2 (Fig. 7). The composition of Unoperated nerves with respect to axon-myelin space, interspace, and debris was consistent among three samples.

Distal to the lesion, at 7–14d PO (n=3), PEG-fused nerve areas were 8±2%, axon, 19±8% myelin, 10±6% debris, and 63±3%, interspace (Fig. 7). In contrast, at 7–14d PO Negative Control nerves had no intact axon or myelin. Debris and interspace composed 46±1% and 54±2% of the area respectively. At 21d PO (n=3), PEG fused nerves areas were 10±7% axon, 10±6% myelin, 12±6% debris, and 68±6% interspace. In contrast, Negative Control nerves were composed of 1±0% axon, 2±0% myelin, 9±5% debris, and 88±4% interspace.

At 42d PO (n=3), PEG fused nerves were composed of 11 ±6% axon, 14±4% myelin, 12±6% debris, and 63±12% interspace. In contrast, Negative Control nerves were composed of 6±4% axon, 9±3% myelin, 11 ±4% debris, and 74±5% interspace.

In summary, in PEG-fused nerves, there were intact axons at all PO times and the area consisting of axon-myelin space increased from 7– 42d PO. In Negative Control nerves, *no axons were seen at 7–14d PO (n=7);* the percent of axon-myelin area increased from 21 (n=2) to 42d PO (n=4) but was always significantly less than PEG-fused nerves. Furthermore, perineurial tissue and fascicles were often observed in Unoperated and most PEG-fused nerves, but not in Negative Control nerves. Capillaries in Unoperated nerves have open lumens, continuous basal lamina, and occasional red blood cells. Most PEG-fused nerves had capillaries with normal to slightly thickened endothelium with less distinct basal lamina and occasional macrophages in near proximity at earlier times. In contrast, all Negative Control nerves had cells radiating from their capillaries at 7 and 21d PO.

Morphological evidence that PEG-fusion produces axonal continuity and reduces or prevents Wallerian degeneration: Neuromuscular junctions (NMJs) and muscle fibers

Figure 9 shows representative confocal images from soleus muscles in Unoperated, PEG-fused, and Negative Control animals at 7 and 21d PO, and TEM images of synaptic clefts 42d PO. Muscle fibers in Unoperated animals were innervated by a single axon (Fig. 9a,d) at a rate of >99% (Table 2), as observed in other muscles in our lab and in other studies (Gutmann and Young, 1944; Miledi and Slater, 1968; Sanes and Lichtman, 1999). Axons branched as they entered AChRs, (Fig. 9: arrows) and mirrored the shape of the AChRs with a high degree of fidelity (Fig. 9d). At the ultrastructural level, pre-synaptic nerve terminals in the synaptic cleft were always directly opposite post-synaptic secondary folds (Fig. 9g, asterisks), muscle fibers had well-organized myosin filaments, sarcoplasmic reticulum, normal mitochondria, and nerve terminals capped by terminal Schwann cell processes (Fig. 9: TSC).

At 7–14d PO, 80% (123/155 synapses, n=2 muscles) of soleus muscles fibers in PEG-fused animals were innervated and nerve terminals usually mirrored the shapes of the AChRs. Sprouting of the nerve terminal was often observed (thin arrow). In contrast, labeled nerves were not observed in Negative Control muscles at 7–14d PO.

At 21d PO, 78% of soleus muscle fibers in PEG fused animals were innervated (118/151 receptors, n=3), often multiply innervated (double arrowhead). In Negative Control muscles, a few very small diameter axons were sometimes observed near labeled receptors, but none occupied AChRs (0/127 receptors, n=2 muscles). Negative Control muscle fibers at 14d PO were significantly smaller than Unoperated muscle fibers (Table 2).

At 42d PO, most NMJs in PEG-fused animals had generally normal ultrastructure and were capped by terminal Schwann cells. At some synapses, axon debris was engulfed by a terminal Schwann cell alongside normal nerve terminals (Fig. 9h: open star). In soleus muscles distal to the transection in Negative Control nerves at 42d PO, most secondary folds were apposed by terminal Schwann cells but nerve terminals were not present (Fig. 9i). Muscle fibers in PEG-fused animals were ultrastructurally normal, but muscle fibers from Negative Control rats were atrophied, poorly organized ultrastructurally, and often showed abnormal mitochondria. Soleus muscle fibers of PEG-fused animals were smaller than Unoperated rats ($p < 0.001$), but significantly larger than those of Negative Control animals ($p < 0.001$).

Note that the presence of innervated NMJs at all PO times for PEG-fused animals correlates well with the functional presence of CAPs, CMAPs (Fig. 1) and muscle twitches at all PO times and their morphological absence in TEM correlates with their functional absence at 0 – 21d PO in Negative Control animals.

Correlations between morphometric and behavioral (SFI) measures in Unoperated, PEG-fused and Negative Control

As would be expected for a positive control in which all animals had SFI scores within the normal range, there was no correlation between SFI measures in Unoperated rats and morphometric measures of sciatic nerve axonal or fiber diameters, axonal density, % NMJ innervation, or muscle fiber area. Figure 10a,b (filled circle symbols) plots such correlations between SFI scores and axonal diameter or axonal density, respectively. As would be expected for a negative control in which all animals showed no significant return of function, there was no correlation between SFI measures in Negative Control rats and morphometric measures of sciatic nerve axonal or fiber diameters, axonal density, % NMJ innervation, or muscle fiber area at 42d PO. Figure 10a,b (x symbol) plots such correlations between SFI scores and axonal diameter or axonal density, respectively. There was also no significant ($p > 0.05$) correlation between SFI measures and any of these morphometric measures for PEG-fused nerves at 42d PO. Figure 10a,b (open circle symbols) plots such correlations between SFI scores and axonal diameter or axonal density, respectively. A significant ($p < 0.05$) correlation was seen between SFI scores and several morphometric measures for allografts having more animals sampled at 42d PO (see Mikesh et al., 2018).

Discussion

Summary of results

Experimental animals having single cuts subsequently repaired with PEG-fusion exhibit:

1. **1**Axolemmal and axoplasmic continuity that is rapidly (within minutes) restored as assessed by conduction of CAPs across the PEG-fused lesion site (Fig. 1a–c), and by CMAPs recorded from muscle groups distal to the lesion (Fig. 1 d–f). [Other publications have also shown diffusion of intra-axonal dyes across the lesion site (Bittner et al., 2012; Ghergherehchi et al., 2016)].

2. **2**Distal segments of singly-transected axons that are continuously maintained from 0-42d PO, i.e., reducing or preventing axonal Wallerian degeneration as assessed by gross anatomical inspection (Fig. 3) and TEM of axonal cross sections (Figs. 4–9, Table 2) of myelinated axons (Figs. 4–7) and of the entire sciatic nerve (Fig. 8).

3. **3**NMJs that are continuously maintained, as measured by CMAPs (Fig. 1 d–f) confocal immunohistochemistry (Fig. 9), TEM (Fig.9) and counts of innervated muscle fibers (Table 2).

4. **4**Muscle fibers that are continuously maintained and routinely undergo very little atrophy (compared with controls), as assessed by TEM (Fig. 9; Table 2).

5. **5**Functional/behavioral recovery that is restored within days to weeks and approaches or equals that of Unoperated animals as measured by the SFI (Fig. 2, Table 2). We always assess nerve repair and define success thereof by behavioral measures, not axon counts nor any other morphological or electrophysiological measure, as Brushart (2011) has emphasized.

Note that PEG-fused distal stumps continuously have many ultrastructurally intact larger and smaller diameter myelinated axons and NMJs that produce CAPs, CMAPs, and muscle twitches at all times tested from 0–42d PO and significant behavioral recovery by at least 14d PO. PEG-fused distal stumps have some axons showing Wallerian degeneration at 7–42d PO and some smaller diameter myelinated axons appearing at 42d PO. In contrast, singly-transected Negative Control axons that are not PEG-fused do ***not*** exhibit any the phenomena 1– 5 above for 7–21d PO and show comparatively little recovery at 42d PO. These minimal recoveries are almost-certainly due to small-diameter myelinated axons regenerating by outgrowth from the severed proximal stumps, of which some may reach denervated target organs at 42d PO, as observed for allograft Negative Controls in the following paper (Mikesh et al., 2018).

Comparisons of our results to previous studies of PEG-fusion

In prior studies (Bittner et al., 2012, 2016a,b; 2017a,b; Rodriguez-Feo et al., 2013; Ghergherehchi et al., 2016; Bamba et al., 2016a, 2017; Riley et al., 2017), single complete transections of the sciatic nerve in the mid-thigh of rats were repaired by neurorrhaphy followed by PEG-fusion or by neurorrhaphy and a Negative Control protocol that used all PEG-fusion solutions *except* the one containing PEG. Immediate effects within minutes to hours of PEG-fusion were characterized by CAPs and/or diffusion of intra-axonal dyes across the PEG-fused lesion site followed by behavioral studies. These data are consistent with the first report of PEG-fusion repair (without neurorrhaphy) of rat sciatic axons by Lore et al (1999, Figures 2 and 4) showing TEM longitudinal sections and intracellular fluorescent dye labeling demonstrating axolemmal and axoplasmic continuity of some PEG-fused axons across the lesion site. In Negative Control animals, intracellular dyes do not diffuse and CAPs do not conduct across the microsutured lesion site in minutes to hours after repair. Neither PEG-fused or Negative Control animals show changes in behavior from 1–3d PO, but over the subsequent 7-≥42d PO, the SFIs in rats with PEG-fused sciatic nerves showed dramatic improvement, often reaching scores typical of animals with intact or sham operated sciatic nerves. SFI scores for animals with PEG-fused sciatic nerves typically approached a plateau value at 42d PO, i.e., usually showed little improvement for months thereafter (see Fig. 1c and Bittner et al., 2012, 2016a,b; 2017a; Ghergherehchi et al., 2016; Bamba et al., 2016a, 2017). In contrast, Negative Control animals rarely attained SFI scores of −70 by 42d PO. Like those of PEG-fused animals, Negative Control SFIs also reached a plateau at about 42d and showed little improvement for months thereafter (Fig. 1d and Bittner et al., 2012, 2016a,b; 2017a,b; Ghergherehchi et al., 2016; Bamba et al., 2016a, 2017; Riley et al., 2017). These previous studies suggested that maintained survival of PEG-fused nerves was responsible for the remarkable recovery of SFI functional/behavioral scores obtained at 7–42d PO, but never demonstrated axon survival in PEG-fused nerves, their absence in Negative Control nerves, or the possible contribution of naturally-occurring outgrowth from severed, surviving axons proximal to the lesion site.

For sciatic nerves singly and completely transected in the mid-thigh of rats, we have now extensively examined various measures that characterize the structure and/or function of axons, myelin, neuromuscular junctions and muscle fibers for 0– 42d PO in PEG-fused and Negative Control animal groups, as well as for intact nerves in Unoperated animals. Our data confirm that, within minutes, PEG-fusion returns axolemmal and axoplasmic continuity for many axons from proximal to distal as measured by CAP conduction across the lesion site (Fig. 1a). Furthermore, fused axons and their motor targets are immediately functional, as assessed by the ability of sciatic nerve stimulation *proximal* to the lesion to evoke CMAPs and muscle twitches *distal* to the lesion (Fig. 1d). This immediate restoration of axonal and neuromuscular function is not associated with much restoration of behavioral function at 3d PO, as assessed by the SFI, consistent with previous reports (Fig. 2). In contrast for Negative Control nerves, we confirm that CAPs are not immediately restored (Fig. 1a) and now also show that CMAPs and muscle twitch are also not evoked (Fig. 1d). We also confirm little or no restoration of behavioral function at 3d PO. [Note that PEG-fused or Negative Control animals cannot be appropriately tested by the SFI while recovering from anesthetics for several days PO (Bittner et al., 2012; Ghergherehchi et al., 2016).]

Our more extensive data confirm that many axons are continuously maintained (survive) from 7d – 42d PO in rats with PEG-fused sciatic nerves, i.e., PEG-fusion prevents Wallerian degeneration of many axons. Many larger diameter axons with intact myelin and NMJs are observed in PEG-fused sciatic nerves that generate CAPs and CMAPs when sampled at 7–42d PO. Postsynaptic muscle fibers are innervated by relatively normal-appearing NMJs from 7–42d PO (Fig. 9 and Table 2) and exhibit significantly less atrophy than muscle fibers in Negative Control animals. Significant behavioral recovery as measured by the SFI routinely occurs within 21d PO in PEG-fused animals, and sometimes approaches levels seen in Unoperated animals by 42d PO (Fig. 2). These maintained axons are almost-certainly axons that were PEG-fused as opposed to regenerating axons, the only other credible explanation compared to assuming activation without neuronal innervation.

However, PEG-fused, maintained axons undergo some changes from their original intact state. For example, CAPs and CMAPs recorded at 7d–42d PO have slower conduction velocities and smaller amplitudes than CAPs or CMAPs from intact nerves. While myelinated axons and innervated NMJs are present at all sampling times from 7d – 42d PO, axon and fiber diameter and myelin in PEG-fused nerves are often smaller and thinner than in Unoperated nerves (Table 2, Figs. 5–8). The number of smaller diameter axons increases in PEG-fused nerves at 21d and 42d PO (Table 2, Figs. 4–9), almost certainly due to some fibers regenerating by outgrowth from the proximal stump that have reached the distal portion of the sciatic nerve in the thigh, but have not yet reached their target muscles (see following paragraph). Average cross-sectional area of muscle fibers is significantly greater than their areas in Negative Control animals, but significantly smaller than their areas in Unoperated animals.

In contrast, Negative Control animals have **no** surviving distal axons at 7, 10, and 14d PO and no detectable NMJs from 7– 21d PO, i.e., all severed axons undergo Wallerian degeneration of their distal processes in Negative Control sciatic nerves. Negative Control nerves have much more debris than Unoperated or PEG-fused nerves at 7d PO [Unoperated nerves essentially have no debris]. That debris is largely removed by 21d PO and remains at about the same level at 42d PO. A few small intact nerve fibers are usually observed distal to the lesion at 21d PO, none of which innervate soleus NMJs. Many more small-diameter myelinated nerve fibers are seen distally at 42d PO. These small diameter myelinated axons are almost-certainly axons regenerating by outgrowth from surviving proximal axonal stumps, a few of which may re-innervate distal muscle masses by 42d PO. Negative Control animals typically show minimal, if any, behavioral recovery by 42d PO, as measured by the SFI test compared to their SFI scores at 3d PO or to SFI values when a 5–10mm segment of sciatic nerve is ablated (Riley et al., 2015; Mikesh et al., 2018). These data are consistent with other reports that transected axons undergo Wallerian degeneration within 7 days and then slowly regrow at ~1mm/day to sometimes reinnervate denervated muscles after a month or more (Brushart, 2011).

Qualitatively similar results are obtained for PEG-fused and Negative Control animals after completely ablating a 5–10mm segment of a sciatic nerve and inserting an autograft or allograft to bridge the nerve gap (Sexton et al., 2012; Riley et al., 2015; Mikesh et al., 2018). These data are also similar to data published by Thayer and his collaborators for single cut (Bamba et al., 2016a, 2017; Sexton et al., 2015; ; Riley et al., 2017,) and to de Medinaceli (1983) who, perhaps inadvertently, used other fusogens in a study designed to test a device to microsuture very carefully trimmed nerve ends after a single transection.

Some hypotheses that might explain results from these PEG-fused sciatic nerves

The data described above might be explained by hypothesizing that PEG-fusion immediately re-establishes axonal continuity for some axons within the nerve that are maintained thereafter, and that NMJs are functionally reinnervated, but not all appropriately activated for 14–42d PO. In this scenario, central and/or peripheral reorganization of non-specifically PEG-fused axons observed in possible combination with slow natural regeneration of axons not PEG-fused (which could also undergo central reorganization) would explain the time lag between immediate neuronal reinnervation within minutes and extensive behavioral restoration within weeks. Our data in this study and a subsequent paper on PEG-fusion of allografts (Mikesh et al., 2018) consistently support this hypothesis. That is, immediately after PEG-fusion and at all times tested to 42d PO, axons continue to conduct action potentials, release transmitter to generate end plate potentials that cause distal muscles to contract as evidenced by CAPs, CMAPS, and muscle twitches. Nerve terminals occupy AChRs at all PO times, even in the absence of SFI recovery. NMJ innervation is maintained as evidenced by CMAPS and improving SFI scores that require an increasing recruitment of more appropriately coordinated muscle contractions, as well as TEM assessments of axonal, myelin, NMJ and muscle structure. We have noted features in electron micrographs of NMJs after PEG fusion closely resemble those found in synaptic competition during development (Fig. 9h; Smith et al., 2013).

As one alternate hypothesis, immediate non-specific PEG-fusion of axons might produce non-functional NMJs, or nerve terminals retract and regrow, and then become functional after several weeks. However, if nerve terminals withdrew or became non-functional, CMAPS should not be recordable in PEG-fused animals at 7d PO or display high rates of muscle fiber innervation (Fig. 1, Table 2). PEG-fusion might produce immediate axonal continuity, but PEG-fused and non-PEG-fused axons might then rapidly (Wallerian) degenerate within 3d –7d PO, followed by enhanced classical axonal outgrowth from the proximal stump (compared to outgrowth in Negative Control animals) to re-innervate denervated muscle masses within several weeks. We think this unlikely, as our data are consistent with the hypothesis that the rate (~1mm/d), extent, and morphology of regenerating axons in PEG-fused nerves is very similar to that observed for Negative Control nerves for at least 42d PO. To achieve reinnervation by regeneration via outgrowth from surviving proximal stumps with the sciatic nerve composition we report, PEG-fused nerves would have to undergo complete debris clearance by 7d PO and accelerate nerve outgrowth to rates approaching 40mm/day for soleus NMJs to display a high degree of nerve re-innervation at 7d PO (73% – 90% in Table 2). These data are important because some researchers (Robinson and Madison, 2016a, b) have assumed that all dye-labeled axons innervating a denervated muscle at 42 or more days after attempting femoral nerve PEG-fusions have arisen by "natural" regeneration via proximal outgrowth. Our data in this and the accompanying paper strongly suggest that many (perhaps most or all) of the axons they dye-labeled are PEG-fused axons that are maintained from 0d to > 42d PO.

Comparisons with other data on neurorrhaphy of singly-cut PNIs

Many papers have examined unoperated intact nerves and nerve regeneration by outgrowth from surviving proximal stumps after transecting major peripheral nerves in rat (de Medinaceli, 1995, MacKinnon et al., 1991, Ikeda and Oka 2012), rabbit (Gutmann and Sanders, 1943), and cat (Arbuthnott et al., 1980; Berthold et al., 1983) model systems. These data consistently show that unoperated mammalian nerves have nerve fiber diameters of 1-15μm. Wallerian degeneration after severance results in degeneration of all myelinated fibers and muscle synapses distal to the lesion within several days. Over the course of weeks to months, smaller diameter (1–5μm) unmyelinated fibers enter the distal stump, enlarge somewhat and form myelin sheaths, but do not exhibit large diameter fibers. For example, MacKinnon et al. (1991) report axon diameters averaging 45% and 70% of unoperated diameters at 30d and >700d after rat sciatic nerve section, respectively. Ikeda and Oka (2012) show that most nerve fibers have diameters of 1–3μm and none larger than 7μm 50d after sciatic nerve transection, with only slight increases in diameter by 200d PO. All of these data and our data agree with analyses of axons regenerating by outgrowth as reviewed and discussed by Brushart (2011).

Muscles distal to a nerve severance (Gutmann and Young, 1944; Reynolds and Woolf, 1992) are denervated for weeks to many months, depending in part on their distance from the lesion site. Reynolds and Woolf (1992) report rare, faint nerve label in large nerve branches in tibialis anterior and soleus muscles 30 days after a sciatic cut, with widespread, complex networks of labeled nerve that do not effectively activate synapses 60d after sciatic nerve severance. In rabbits, Gutmann and Young (1944) report a 25d delay from the time of peroneal nerve cut to the first signs of axon arrival in the peroneus longus muscle, but no obviously innervated synapses until nearly 60d after injury. The consistent result of these and other studies is that regenerating axons slowly return to denervated synapses after months of denervation and often fail to occupy and/or stimulate the receptor (Brushart et al., 2002, Gramsbergen et al., 2000, Ijkema-Paassen et al., 2002; Sakuma et al., 2016). Our data from Negative Control animals are consistent with these previous reports. We strongly suspect these results also apply to unsuccessfully PEG-fused axons in PEG-fused nerves that subsequently slowly regenerate by outgrowth from surviving PEG sealed proximal stumps.

That is, PEG fuses closely-apposed open axonal ends or, if not closely apposed, seals each shut (thereby preventing PEG-fusion), depending on the experimental protocol (Spaeth et al., 2012; Bittner et al., 2016a,b; 2017a,b).

Micro-crush injuries of major peripheral nerves

It is important to note for experimental animal models that 1–3 mm long micro-crush injuries made with fine forceps to directly pinch a sciatic or other peripheral nerve do not completely disrupt axonal endoneurial sheaths. Subsequent functional/behavioral recoveries are often very good, presumably because axons can regenerate by outgrowths guided to their appropriate original targets by surviving sheaths that contain viable Schwann cells, even though the original distal axonal segments have undergone Wallerian degeneration (Nguyen et al., 2002; Brushart, 2011, Wood et al., 2011). For axonal regeneration by outgrowth at ~1mm/d, good motor and/or sensory recoveries tissue measured by the SFI and other tests often occur within weeks to months PO, depending on the distance between the injury site and denervated target. PEG-fusion may slightly increase the rate of behavioral recovery for 1–2mm micro-crushes of rat sciatic nerves in mid-thigh (Britt et al., 2010; Bittner et al., 2012). Such micro-crushes do not occur by naturally occurring traumas in larger mammals, including humans.

Extensive CNS and PNS plasticity explains dramatic behavioral recovery after PEG-fusions

Although our data on the structure and function of peripheral axons, NMJs and muscle fibers are best explained by PEG-fusion immediately re-establishing axonal continuity and maintenance thereafter, they do not explain the cellular or systems (much less molecular) mechanisms by which these surviving PEG-fused axons produce their dramatic functional/behavioral recovery within weeks. We suggest that this behavioral recovery is explained at least in part by extensive reorganization of PEG-fused motoneurons, and may be described as ‘multiple realizability’ (Krakauer et al., 2017). This extensive reorganization is demonstrated by one of our previous papers (Bittner et al., 2017b) and by the data reported by Robinson and Madison (2016), although they interpreted their result as resulting from inappropriately directed, non-specific reinnervation by motoneurons regenerating by outgrowth from surviving proximal stumps (Robinson and Madison, 2016).

Conclusions

The principle aim of this work was to describe morphological and functional outcomes to accompany our behavioral assessments and provide a foundation for a more complete understanding of this novel cellular repair system. Our results strongly suggest that PEG-fusion maintains innervation of motor synapses, prevents extensive atrophy of muscle fibers distal to a complete nerve transection, and enables recovery. These results are consistent with the hypothesis that PEG-fusion immediately re-establishes and then maintains axonal continuity for many axons and NMJs remain functionally reinnervated, but not appropriately activated until 14– 42d PO.

The results of PEG-fusion contradict much current Neuroscience dogma that asserts that: (**1**) distal stumps of severed axons must undergo Wallerian degeneration within days and (**2**) reinnervation only occur by regenerating outgrowths from severed proximal stumps that need appropriately reinnervate denervated target tissues. In contrast, our PEG-fusion results show that: (**1**) distal stumps of PEG-fused severed axons survive indefinitely, (**2**) PEG-fusion induces reinnervation within seconds to minutes by connecting axons in proximal and distal stumps to appropriately or inappropriately reinnervate denervated target tissues, and (**3**) dramatic behavioral recovery must be due to inappropriate connections that undergo extensive peripheral and/or CNS plasticities that support functional recovery.

Our results strongly suggest that voluntary behavior is the best measure of recovery success after nerve transection followed by PEG-fusion, neurorrhaphy or other restorative procedures. Other measures such as the ratio of myelin thickness to axon diameter (r=0.53, de Medinaceli, 1995) or axon numbers (Mackinnon et al., 1991; Brushart, 2011) do not correlate well with behavioral recovery, with the possible exception of axon or nerve fiber diameter (see Mikesh et al., 2018).

Finally, transection of peripheral nerves often results in long-term disability. To date, several pilot clinical case studies strongly suggest that PEG-fusion indeed produces very favorable outcomes (Bamba et al., 2016b; cf. Robinson and Madison, 2016). That is, use of PEG-fusion in conjunction with neurorrhaphy for single-cut injuries has the potential to greatly reduce the PO time between surgical repair of a severed nerve and beginning to recover sensation or motor control and to dramatically increase the eventual extent of functional recovery. To accomplish these remarkable results, the PEG-fusion repair must be made before Wallerian degeneration occurs in the distal stump somewhere between 1–3 days. Bamba et al. (2017) have recently reported that this interval is at least 36h. We have shown that this interval might be extended to 5–10 days by cooling axons *in vitro* (Marzullo et al, 2001) or in a body part *in vivo* (Sea et al, 1995) or by *in vivo* treatment with Cyclosporin A (Sunio et al, 1997). That is, surgeons might have 5–10 days after a PNI to repair it by PEG-fusion.

Acknowledgments

We wish to thank the Microscopy and Imaging Facility of the Center for Biomedical Research Support at The University of Texas at Austin for access and assistance with confocal and electron microscopy, and the University of Texas Department of Statistics and Data Sciences for consulting services.

Support or grant information: Supported by grants from the Lone Star Paralysis Foundation to GDB, NIH grant R01 NS081063 to GDB and Lone Star Paralysis grant to RCT.

References

Allan CH. Functional results of primary nerve repair. Hand Clin. 2000; 16:67–72. [PubMed: 10696577]

Arbuthnott ER, Boyd IA, Kalu KU. Ultrastructural dimensions of myelinated peripheral nerve fibres in the cat and their relation to conduction velocity. J Physiol. 1980; 308:125–57. [PubMed: 7230012]

Bamba R, Riley DC, Kelm ND, Does MD, Dortch RD, Thayer WP. A novel technique using hydrophilic polymers to promote axonal fusion. Neural Regen Res. 2016a; 11(4):525–528. DOI: 10.4103/1673-5374.180724 [PubMed: 27212898]

Bamba R, Riley DC, Kim JS, Cardwell NL, Pollins AC, Shack RB, Thayer WP. Evaluation of a nerve fusion technique with polyethyelene glycol in a delayed setting after nerve injury. J Hand Surg Am. 2017; pii: S0363-5023(17)31223-6. doi: 10.1016/j.jhsa.2017.07.014

Bamba R, Waitayaawinyu T, Nookala R, Riley DC, Boyer RB, Sexton KW, Boonyasirrikool C, Niempoog S, Kelm ND, Does MD, Dortch RD, Shack RB, Thayer WP. A novel therapy to promote axonal fusion in human digital nerves. J Trauma Acute Care Surg. 2016b; 81(Supplement):S177–S183. DOI: 10.1097/TA.0000000000001203 [PubMed: 27768666]

Berthold CH, Nilsson I, Rydmark M. Axon diameter and myelin sheath thickness in nerve fibres of the ventral spinal root of the seventh lumbar nerve of the adult and developing cat. Journal of Anatomy. 1983; 136:483–508. [PubMed: 6885614]

Bittner GD, Keating CP, Kane JR, Britt JM, Spaeth CS, Fan JD, Zuzek A, Wilcott RW, Thayer WP, Winograd JM, Gonzalez-Lima F, Schallert T. Rapid, effective, and long-lasting behavioral recovery produced by microsutures, methylene blue, and polyethylene glycol after completely cutting rat sciatic nerves. J Neurosci Res. 2012; 90:967–980. DOI: 10.1002/jnr.23023 [PubMed: 22302646]

Bittner GD, Mikesh M, Ghergherehchi CL. PEG-fusion retards Wallerian degeneration and rapidly restores behaviors lost after nerve severance. Neural Regen Res. 2016a; 11:217–219. DOI: 10.4103/1673-5374.177716 [PubMed: 27073362]

Bittner GD, Sengelaub DL, Ghergherehchi CL. Conundrums and confusions regarding how PEG-fusion produces excellent behavioral recovery after peripheral nerve injuries. Neural Regen Res. 2017a; 12doi: 10.4103/1

Bittner GD, Sengelaub DR, Trevino RC, Ghergherehchi CL, Mikesh M. Robinson and Madison have published no data on whether polyethylene glycol fusion repair prevents reinnervation accuracy in rat peripheral nerve. J Neurosci Res. 2017b; 95:863–866. DOI: 10.1002/jnr.23849 [PubMed: 27514994]

Bittner GD, Sengelaub DR, Trevino RC, Peduzzi JD, Mikesh M, Ghergherehchi CL, Schallert T, Thayer WP. The curious ability of polyethylene glycol fusion technologies to restore lost behaviors after nerve severance. J Neurosci Res. 2016b; 94:207–230. DOI: 10.1002/jnr.23685 [PubMed: 26525605]

Bozkurt A, Deumens R, Scheffel J, O'Dey DM, Weis J, Joosten EA, Führmann T, Brook GA, Pallua N. CatWalk gait analysis in assessment of functional recovery after sciatic nerve injury. J Neurosci Methods. 2008; 173:91–98. DOI: 10.1016/j.jneumeth.2008.05.020 [PubMed: 18577402]

Britt JM, Kane JR, Spaeth CS, Zuzek A, Robinson GL, Gbanaglo MY, Estler CJ, Boydston EA, Schallert T, Bittner GD. Polyethylene glycol rapidly restores axonal integrity and improves the rate of motor behavior recovery after sciatic nerve crush injury. J Neurophysiol. 2010; 104:695–703. DOI: 10.1152/jn.01051.2009 [PubMed: 20445038]

Brushart TM, Hoffman PN, Royall RM, Murinson BB, Witzel C, Gordon T. Electrical stimulation promotes motoneuron regeneration without increasing its speed or conditioning the neuron. J Neurosci. 2002; 22(15):6631–6638. doi: 20026683. [PubMed: 12151542]

Brushart, TM. Nerve Repair. NY: Oxford University Press; 2011.

Burch, R. Nerve repair. In: Wolfe, S.Pederson, W.Hotchkiss, R., Kozin, S., editors. Green's operative hand surgery. 6th. NY: Churchill Livingstone; 2011.

Campbell WW. Evaluation and management of peripheral nerve injury. Clin Neurophysiol. 2008; 119:1951–1965. DOI: 10.1016/j.clinph.2008.03.018 [PubMed: 18482862]

Carlton JM, Goldberg NH. Quantitating integrated muscle function following reinnervation. Surg Forum. 1986; 37:611–612.

Cohen, J. Statistical power analysis for the behavioral sciences. NJ: Lawrence Erlbaum Associates; 1998.

Cragg BG, Thomas PK. The conduction velocity of regenerated peripheral nerve fibres. J Physiol. 1964; 171(1):164–75. DOI: 10.1113/jphysiol.1964.sp007369 [PubMed: 14170140]

Cross JD, Ficke JR, Hsu JR, Masini BD, Wenke JC. Battlefield orthopaedic injuries cause the majority of long-term disabilities. J Am Acad Orthop Surg. 2011; 19(Suppl 1):S1–S7. [PubMed: 21304041]

de Medinaceli L, Freed WJ, Wyatt RJ. An index of the functional condition of rat sciatic nerve based on measurements made from walking tracks. Exp Neurol. 1982; 77:634–643. DOI: 10.1016/0014-4886(82)90234-5 [PubMed: 7117467]

de Medinaceli L, Wyatt RJ, Freed WJ. Peripheral nerve reconnection: Mechanical, thermal, and ionic conditions that promote the return of function. Exp Neurology. 1983; 81:469–487. DOI: 10.1016/0014-4886(83)90276-5 de Medinaceli L. Interpreting nerve morphometry data after experimental traumatic lesions. J Neuroscience Methods. 1995; 58:29–37. DOI: 10.1016/0165-0270(94)00156-B

Fields DR, Ellisman MH. Axons regenerated through silicone tube splices: II. Functional morphology. Exp Neurol. 1986; 92:61–74. DOI: 10.1016/0014-4886(86)90125-1 [PubMed: 3956659]

Ghergherehchi CL, Bittner GD, Hastings RL, Mikesh M, Riley DC, Trevino RC, Schallert T, Thayer WP, Sunkesula SR, Ha TA, Munoz N, Pyarali M, Bansal A, Poon AD, Mazal AT, Smith TA, Wong NS, Dunne PJ. Effects of extracellular calcium and surgical techniques on restoration of axonal continuity by polyethylene glycol fusion following complete cut or crush severance of rat sciatic nerves. J Neurosci Res. 2016; 94:231–245. DOI: 10.1002/jnr.23704 [PubMed: 26728662]

Gramsbergen A, Ijkema-Paassen J, Meek MF. Sciatic Nerve Transection in the Adult Rat: Abnormal EMG Patterns during Locomotion by Aberrant Innervation of Hindleg Muscles. Exp Neurol. 2000; 161:183–193. DOI: 10.1006/exnr.1999.7233 [PubMed: 10683284]

Green, DP., Wolfe, SW. Green's operative hand surgery. 6th. Philadelphia: Elsevier/Churchill Livingstone; 2011.

Gutmann E, Sanders FK. Recovery of fibre numbers and diameters in the regeneration of peripheral nerves. J Phys. 1943; 101:489–518.

Gutmann E, Young JZ. The re-innervation of muscle after various periods of atrophy. J Anat. 1944; 78:15–43. [PubMed: 17104938]

Ijkema-Paassen J, Meek MF, Gramsbergen A. Reinnervation of muscles after transection of the sciatic nerve in adult rats. Muscle Nerve. 2002; 25:891–897. DOI: 10.1002/mus.10130 [PubMed: 12115979]

Ikeda M, Oka Y. The relationship between nerve conduction velocity and fiber morphology during peripheral nerve regeneration. Brain and Behavior. 2012; 2:382–390. DOI: 10.1002/brb3.61 [PubMed: 22950042]

Kandel, ER., Schwartz, JH., Jessell, TM., Siegelbaum, SA., Hudspeth, AJ. Principles of neural science. 5th. New York: Elsevier; 2013.

Kang H, Tian L, Son YJ, Zuo Y, Procaccino D, Love F, Hayworth C, Trachtenberg J, Mikesh M, Sutton L, Ponomareva O, Mignone J, Enikolopov G, Rimer M, Thompson W. Regulation of the intermediate filament protein nestin at rodent neuromuscular junctions by innervation and activity. J Neurosci. 2007; 27:5948–5957. DOI: 10.1523/JNEUROSCI.0621-07.2007 [PubMed: 17537965]

Krakauer JW, Ghazanfar AA, Gomez-Marin A, MacIver MA, Poeppel D. Neuroscience Needs Behavior: Correcting a Reductionist Bias. Neuron. 2017; 93:480–490. DOI: 10.1016/j.neuron.2016.12.041 [PubMed: 28182904]

Krause TL, Fishman HM, Ballinger ML, Bittner GD. Extent and mechanism of sealing in transected giant axons of squid and earthworms. J Neurosci. 1994; 14:6638–6651. [PubMed: 7965066]

Lentz BR. PEG as a tool to gain insight into membrane fusion. Eur Biophys J. 2007; 36(4–5):315–26. DOI: 10.1007/s00249-006-0097-z [PubMed: 17039359]

Lore AB, Hubbell JA, Bobb DS, Ballinger ML, Loftin KL, Smith JW, Smyers ME, Garcia HD, Bittner GD. Rapid induction of functional and morphological continuity between severed ends of mammalian or earthworm myelinated axons. J Neurosci. 1999; 19:2442–2454. [PubMed: 10087059]

Mackinnon SE, Dellon AL, O'Brien JP. Changes in nerve fiber numbers distal to a nerve repair in the rat sciatic nerve model. Muscle Nerve. 1991; 14:1116–22. [PubMed: 1745287]

Marzullo TC, Britt JS, Stavisky R, Bittner GD. Cooling enhances in vitro survival and fusion-repair of severed axons taken from the peripheral and central nervous system of rats. Neuroscience Letters. 2001; 327:9–12.

Michailov GV, Sereda MW, Brinkmann BG, Fischer TM, Haug B, Birchmeier C, Role L, Lai C, Schwab MH, Nave KA. Axonal neuregulin-1 regulates myelin sheath thickness. Science. 2004; 304(5671):700–3. DOI: 10.1126/science.1095862 [PubMed: 15044753]

Mikesh M, Ghergherehchi CL, Rahesh S, Jagannath K, Ali A, Sengelaub DR, Trevino RC, Jackson DM, Bittner GD. Polyethylene glycol treated allografts not tissue matched nor immunosuppressed rapidly repair sciatic nerve gaps, maintain neuromuscular functions, and restore voluntary behaviors in female rats. J Neurosci Res. 2018 In press.

Miledi R, Slater CR. Electrophysiology and Electron-Microscopy of Rat Neuromuscular Junctions After Nerve Degeneration. Proc R Soc B Biol Sci. 1968; 169:289–306. DOI: 10.1098/rspb.1968.0012 [PubMed: 4384567]

Nguyen QT, Sanes JR, Lichtman JW. Pre-existing pathways promote precise projection patterns. Nat Neuroscience. 2002; 5(9):861–7. DOI: 10.1038/nn905 [PubMed: 12172551]

Reynolds ML, Woolf CJ. Terminal Schwann cells elaborate extensive processes following denervation of the motor endplate. J Neurocytol. 1992; 21:50–66. [PubMed: 1346630]

Robinson GA, Madison RD. Polyethylene glycol fusion repair prevents reinnervation accuracy in rat peripheral nerve. J Neurosci Res. 2016; 94:636–644. DOI: 10.1002/jnr.23734 [PubMed: 26994857]

Robinson GA, Madison RD. The title and data of Robinson and Madison are valid. J Neurosci Res. 2017; 95:867–868. DOI: 10.1002/jnr.23867 [PubMed: 27510502]

Rodriguez-Feo CL, Sexton KW, Boyer RB, Pollins AC, Cardwell NL, Nanney LB, Shack RB, Mikesh MA, McGill CH, Driscoll CW, Bittner GD, Thayer WP. Blocking the P2X7 receptor improves outcomes after axonal fusion. J Surg Res. 2013; 184:705–713. DOI: 10.1016/j.jss.2013.04.082 [PubMed: 23731685]

Riley DC, Bittner GD, Mikesh M, Cardwell NL, Pollins AC, Ghergherehchi CL, Bhupanapadu Sunkesula SR, Ha TN, Hall BT, Poon AD, Pyarali M, Boyer RB, Mazal AT, Munoz N, Trevino RC, Schallert T, Thayer WP. Polyethylene glycol-fused allografts produce rapid behavioral recovery after ablation of sciatic nerve segments. J Neurosci Res. 2015; 93:572–583. DOI: 10.1002/jnr.23514 [PubMed: 25425242]

Riley DC, Boyer RB, Deister CA, Pollins AC, Cardwell NL, Kelm ND, Does MD, Dortch RD, Bamba R, Shack RB, Thayer WP. Immediate Enhancement of Nerve Function Using a Novel Axonal Fusion Device After Neurotmesis. Ann Plast Surg. 2017; doi: 10.1097/SAP.0000000000001242

Rupp A, Dornseifer U, Fischer A, Schmahl W, Rodenacker K, Jütting U, Gais P, Biemer E, Papadopulos N, Matiasek K. Electrophysiologic assessment of sciatic nerve regeneration in the rat: surrounding limb muscles feature strongly in recordings from the gastrocnemius muscle. J Neurosci Methods. 2007; 166:266–77. DOI: 10.1016/j.jneumeth.2007.07.015 [PubMed: 17854904]

Sakuma M, Gorski G, Sheu S-H, Lee S, Barrett LB, Singh B, Omura T, Latremoliere A, Woolf CJ. Lack of motor recovery after prolonged denervation of the neuromuscular junction is not due to regenerative failure. Eur J Neurosci. 2016; 43:451–62. DOI: 10.111/ejn.13059 [PubMed: 26332731]

Sanes JR, Lichtman JW. Development of the vertebrate neuromuscular junction. Annu Rev Neurosci. 1999; 22:389–442. DOI: 10.1146/annurev.neuro.22.1.389 [PubMed: 10202544]

Sawilowsky SS. New Effect Size Rules of Thumb. J Modern Applied Statistical Methods. 2009; 8:26.doi: 10.22237/jmasm/1257035100

Schneider CA, Rasband WS, Eliceiri KW. NIH Image to ImageJ: 25 years of image analysis. Nature Methods. 2012; 9:671–675. DOI: 10.1038/nmeth.2089 [PubMed: 22930834]

Sea T, Ballinger ML, Bittner GD. Cooling of peripheral myelinated axons retards Wallerian degeneration. Exp Neurol. 1995; 133:85–95. DOI: 10.1006/exnr.1995.1010 [PubMed: 7601266]

Sexton KW, Pollins AC, Cardwell NL, Del Corral GA, Bittner GD, Shack RB, Nanney LB, Thayer WP. Hydrophilic polymers enhance early functional outcomes after nerve autografting. J Surg Res. 2012; 177:392–400. DOI: 10.1016/j.jss.2012.03.049 [PubMed: 22521220]

Sexton KW, Rodriguez-Feo CL, Boyer RB, Del Corral GA, Riley DC, Pollins AC, Cardwell NL, Shack RB, Nanney LB, Thayer WP. Axonal fusion via conduit-based delivery of hydrophilic polymers. Hand. 2015; 10:688–694. DOI: 10.1007/s11552-015-9780-9 [PubMed: 26568724]

Sherman DL, Krols M, Wu LM, Grove M, Nave KA, Gangloff YG, Brophy PJ. Arrest of myelination and reduced axon growth when Schwann cells lack mTOR. J Neurosci. 2012; 32(5):1817–25. DOI: 10.1523/JNEUROSCI.4814-11.2012 [PubMed: 22302821]

Smith IW, Mikesh M, Lee Yi, Thompson WJ. Terminal Schwann Cells Participate in the Competition Underlying Neuromuscular Synapse Elimination. J Neurosci. 2013; 33:17724–17736. DOI: 10.1523/JNEUROSCI.3339-13.2013 [PubMed: 24198364]

Spaeth CS, Boydston EA, Figard LR, Zuzek A, Bittner GD. A model for sealing plasmalemmal damage in neurons and other eukaryotic cells. J Neurosci. 2010; 30:15790–15800. DOI: 10.1523/JNEUROSCI.4155-10.2010 [PubMed: 21106818]

Spaeth CS, Robison T, Fan JD, Bittner GD. Cellular mechanisms of plasmalemmal sealing and axonal repair by polyethylene glycol and methylene blue. J Neurosci Res. 2012; 90:955–966. DOI: 10.1002/jnr.23022 [PubMed: 22302626]

Stansbury LG, Branstetter JG, Lalliss SJ. Amputation in military trauma surgery. J Trauma. 2007; 63:940–944. DOI: 10.1097/TA.0b013e31814934d8 [PubMed: 18090027]

Sunio A, Bittner GD. Cyclosporin retards the Wallerian degeneration of peripheral mammalian axons. Exp Neurol. 1997; 146:46–56. DOI: 10.1006/exnr.1997.6484 [PubMed: 9225737]

Wolthers M, Moldovan M, Binderup T, Schmalbruch H, Krarup C. Comparative electrophysiological, functional, and histological studies of nerve lesions in rats. Microsurgery. 2005; 25:508–519. DOI: 10.1002/micr.20156 [PubMed: 16145683]

Wood MW, Kemp SWP, Weber C, Borschel GH, Gordon T. Outcome measures of peripheral nerve regeneration. Ann Anat. 2011; 193:321–333. DOI: 10.1016/j.aanat [PubMed: 21640570]

Significance Statement

PEG-fusion of completely-severed rat sciatic nerves prevents much Wallerian degeneration, rapidly restores action potential conduction across the lesion site, and maintains nerve/muscle structures and functions. Lost behaviors are restored within days to weeks, often to levels observed for unoperated/intact sciatic nerves. These results are due to motor and/or sensory axonal PEG-fusions that are very nonspecific with respect to the originally innervated targets. Axons regenerating by naturally-occurring outgrowths from surviving proximal axonal cut ends contribute little to this behavioral recovery. Adoption of this PEG-fusion technology could produce a paradigm shift from current clinical practice to repair complete transections solely by neurorrhaphy.

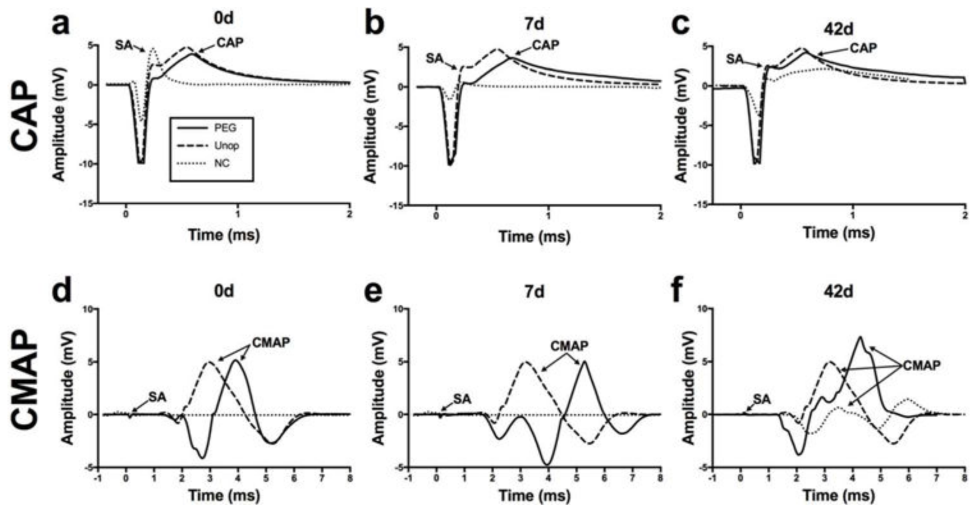

Figure 1.

Representative CAPs (a,b,c) and CMAPs (d,e,f) from intact, PEG-fused and Negative Control singly transected sciatic nerves at 0d PO (a,d), 7d PO (b,e) and 42d PO (c,f). Panels a,d: SA: stimulus artifact; Unop: unoperated and intact nerve before lesioning (dashed line in all panels; NC: Negative Control nerves after microsuturing and all solutions applied except PEG (dotted line in all panels); PEG: microsutured, PEG-fused nerve (solid line in all panels). The same abbreviations are used in other figures. Panels b,c and e,f: the CAP or CMAP recorded from the originally-intact nerve is plotted to give a “baseline reference response” to compare visually with CAPs and CMAPs recorded from PEG-fused and Negative Control nerves at 7d and 42d PO, respectively.

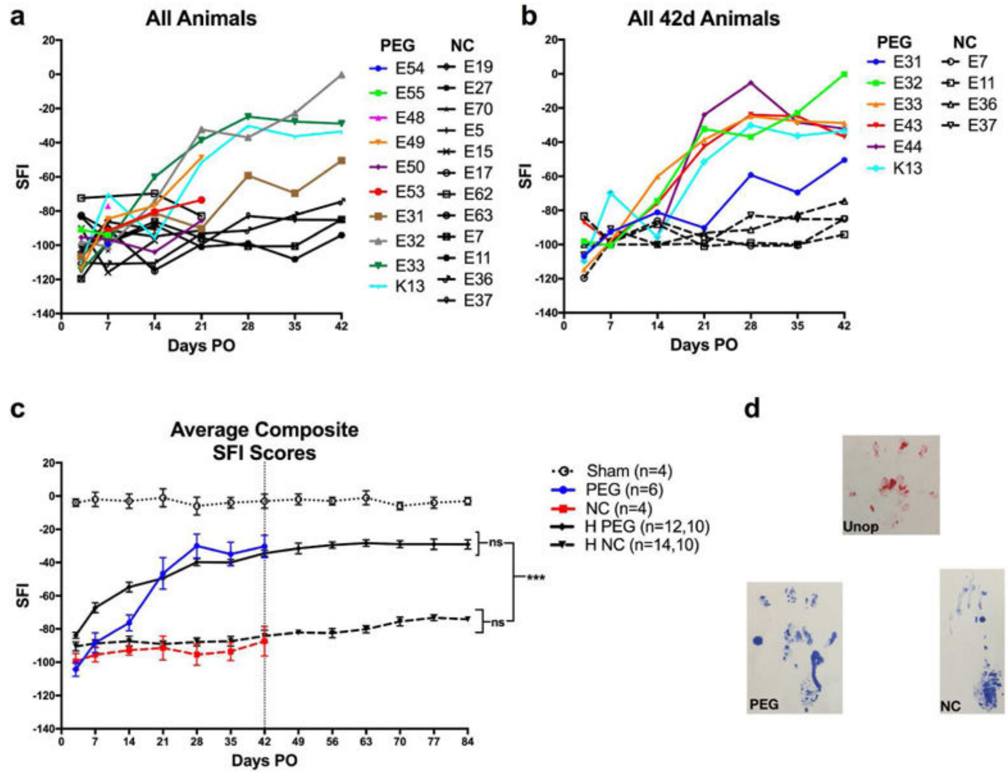

Figure 2.

SFI scores (a,b,c) vs. PO days and (d) paw prints for all PEG, NC, or sham-operated (sham) individual. SFI scores from 3d to 42d PO of all individual rats (see key and Table 2) receiving a PEG-fused (PEG) or Negative Control (NC) transection. HPEG = Historical + current PEG-fusion animals all using the current PEG-fusion protocol. HNC = Historical + current Negative Control animals all using the current Negative Control protocol. Note that animals sacrificed for morphometric analyses are no longer available to be behaviorally tested (a). SFI scores from all PEG and Negative Control individual rats tested from 0d–42d PO. Average ± SE SFI for animals used in this study (colored lines and points) and our historical average (black lines and points) for PEG-fused and Negative Control animals that received the same PEG-fusion protocol described herein. The two n values in the key for each curve gives the number of animals sampled at 3d–42d PO and the number animals that continued to be sampled at 49d –84d PO, respectively. Vertical bar marks 42d PO for which vertical bars and asterisks at right of graphs bars show p value comparisons *,**,*** = $p <$ 0.05, 0.01, and < 0.001, respectively; ns = not significant ($p > 0.05$). p values in other figures use the same asterisk and ns symbolic designations.

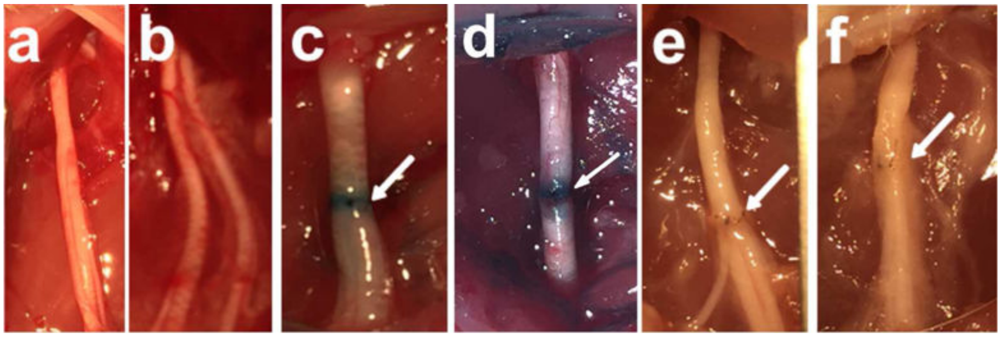

Figure 3.

Images taken through a surgical microscope. Unoperated intact sciatic nerves (a,b), 0d single cut PEG-fused sciatic nerve (c), 0d single cut Negative Control (d), 42d single cut PEG (e), 42d single cut Negative Control (f). Arrows point to site of neurorrhaphy.

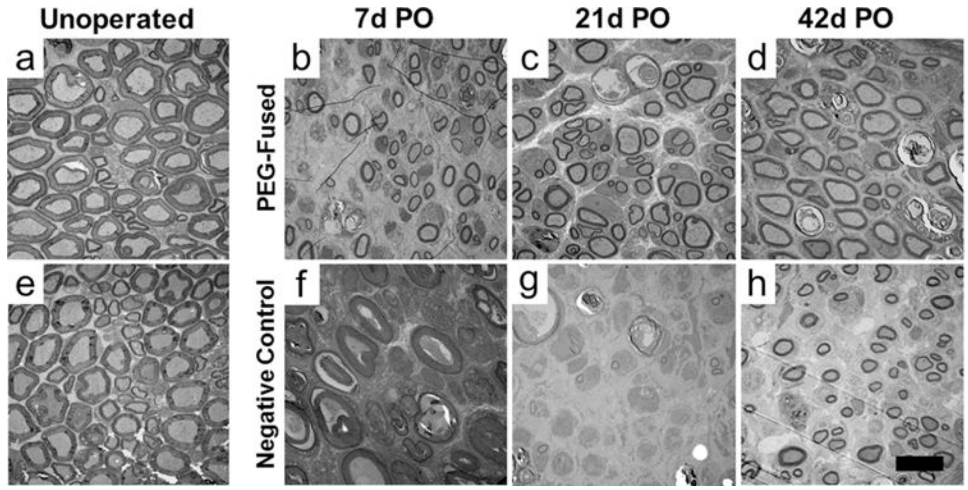

Figure 4.

TEM cross sections of unoperated, intact sciatic axons in the proximal (a) and distal (e) thigh of rats and transected PEG-fused (b – d) or Negative Control distal axons (f – h) at 7d (b,f), 21d (c,g) and 42d (d,h) PO. Scale bar = 10μm.

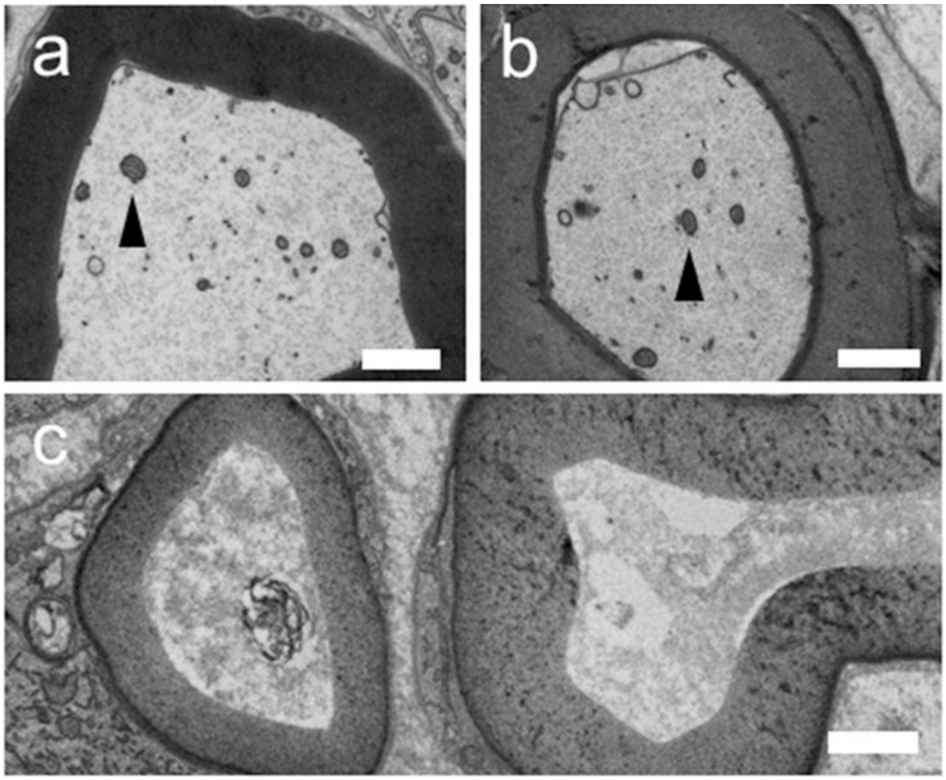

Figure 5.
Higher power TEM of a) Unoperated axon, b) 10d PO PEG fused axon distal to a single transection injury, c) 10d PO Negative Control axon distal to a single transection injury. Arrow heads point to mitochondria.

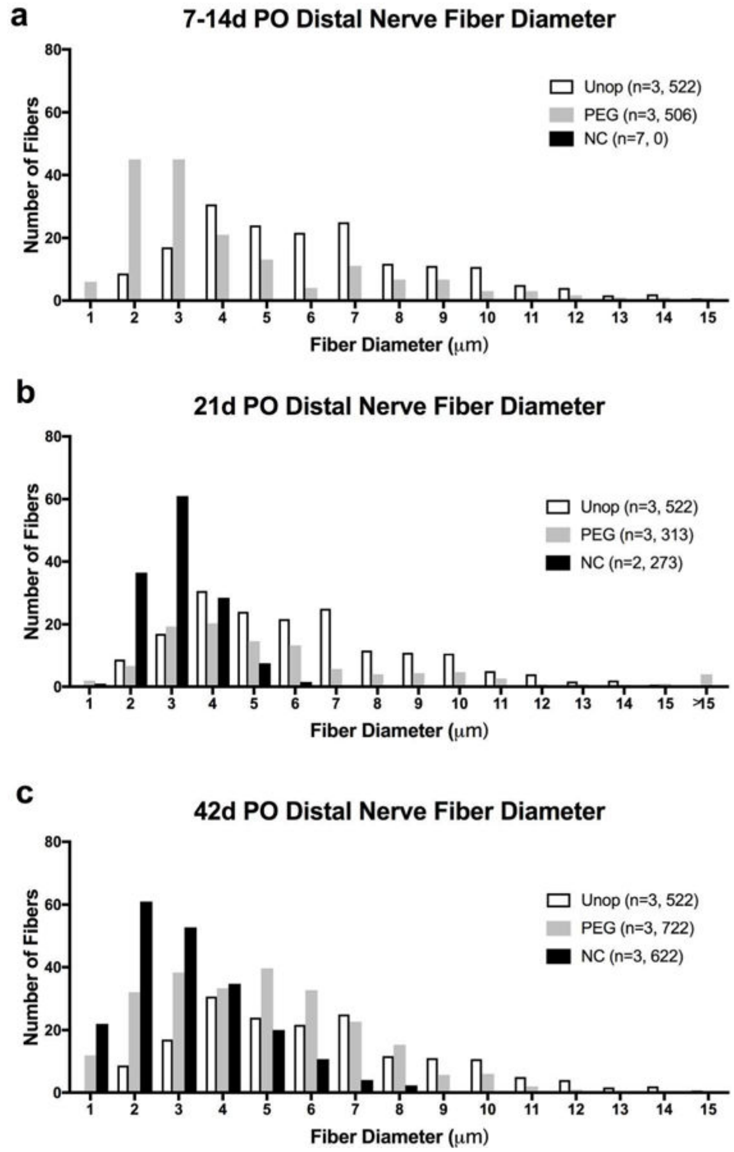

Figure 6.

Histograms of nerve fiber diameters versus average number of fibers per 10,000μm2 for a sciatic nerve. Bin width is 1μm (1– 1.99μm, 2– 2.99μm, etc.) for Unoperated (Unop) nerve never transected and for PEG-fused (PEG), and Negative Control (NC) distal nerve stumps at 7–14d, 21d, and 42d PO. PEG-fused axons increase in diameter from 7 to 42d and maintain a wide range of fiber diameters. Negative Controls have a narrow range of small axon diameters at 21d and 42d PO. n = total number of sciatic nerves, total number of nerve fibers measured. NC* = no intact axons present at 7–14d PO in Negative Control nerves.

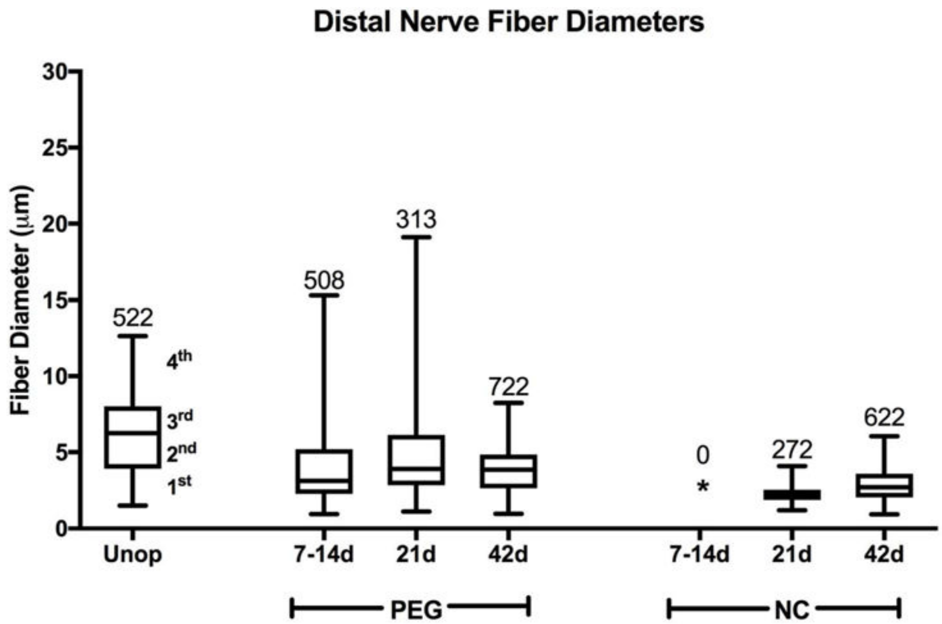

Figure 7.

Box plots showing range of nerve fiber diameters (µm) for each quartile. Plots show range of fiber diameters in Unoperated (Unop) sciatic nerves and in PEG-fused (PEG) and Negative Control (NC) sciatic nerves at 7–14d, 21d, and 42d PO for transected nerves 6mm distal to the lesion site. The line separating the 2nd and 3rd quartiles shows the median diameter. * signifies no surviving axons. Numbers at the top of the highest quartile give total number of nerve fibers counted for that protocol at that time (also see Table 2). Note that PEG-fused fiber diameters more closely resemble Unoperated than Negative Control diameters and that no Negative Control axons are present at 7–14d PO.

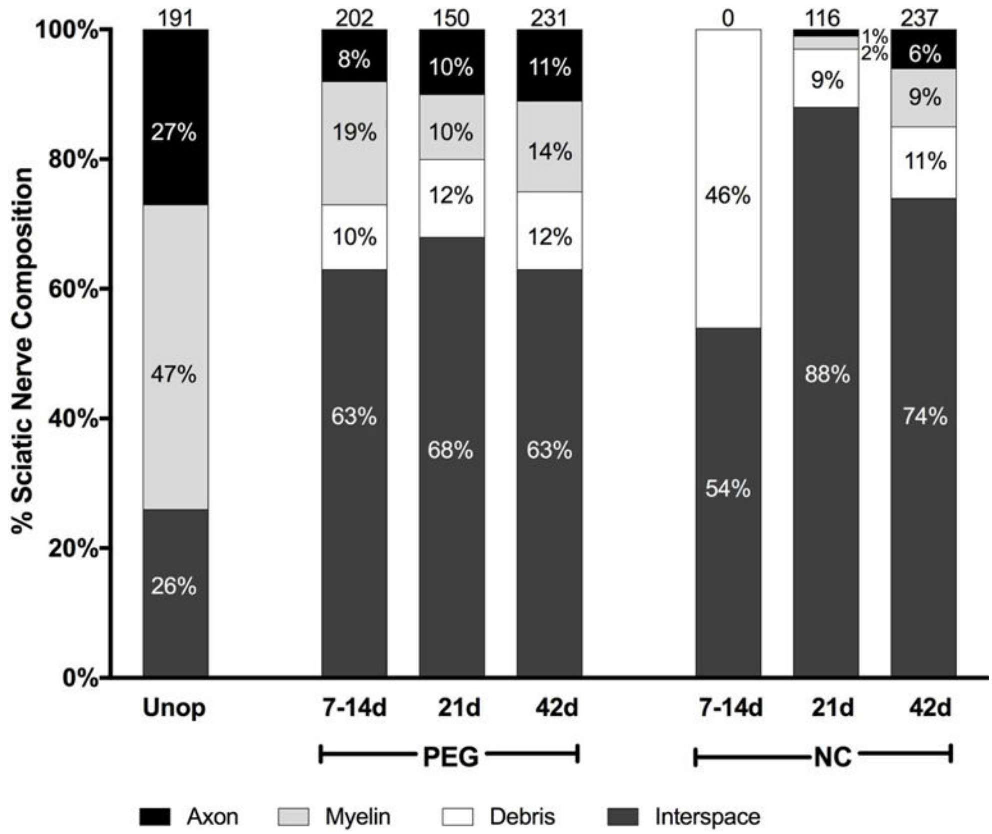

Figure 8.

Composition of sciatic nerves for Unoperated or singly-transected PEG-fused and Negative Control nerves distal to the lesion at 7–14d, 21d, and 42d PO. Amount (%) of total sciatic nerve area consumed by axons, myelin, degradation debris, and intercellular space (see text for definitions). Numbers at the top of the bar graphs denote axons per 10,000µm2.

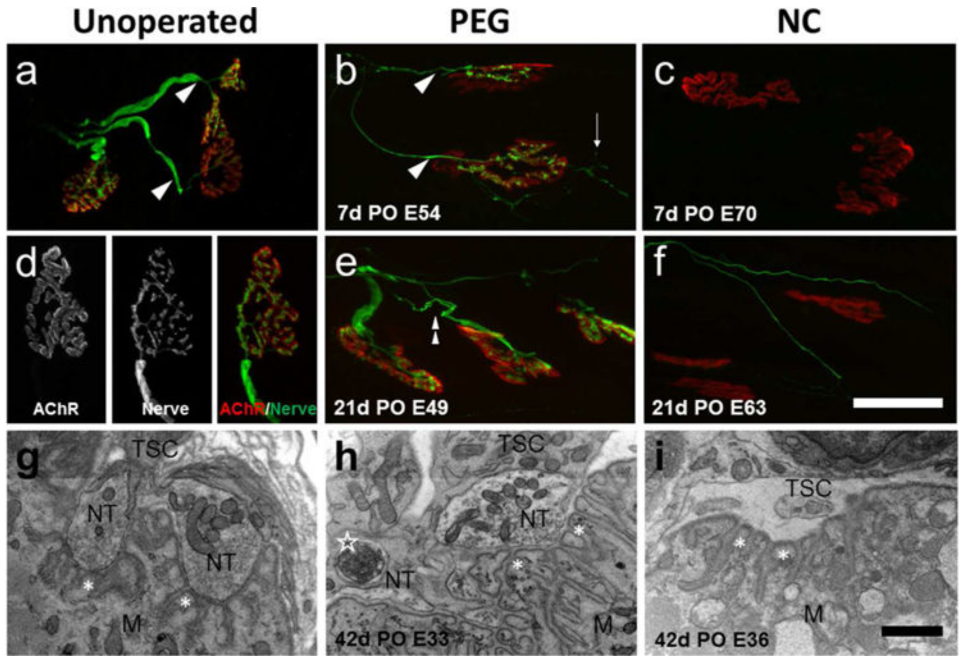

Figure 9.

Confocal and TEM images of soleus NMJs. Unoperated (a,d), singly cut PEG-fused (b,e), and negative control (NC) (c,f) animals at 7 and 21d PO, showing SV2 and 2H3 labeled axons (green) and bungarotoxin labeled AChRs (red). Scale bar a–c, e,f = 50µm. g,h,i: TEM images of soleus NMJs from Unoperated (g), PEG-fused (h), and Negative Control (i) at 42d PO. Scale bar g–i = 2µm. Confocal images show robustly labeled nerve terminals directly apposed to their AChRs in both the Unoperated and 7 and 21d PO PEG-fused NMJs, but only a few thin axons in the 21d NC. These regenerating axons do not make contact with post-synaptic receptors. In a–f, arrowheads = single innervation, thin arrows = nerve terminal sprouts, double arrowhead = multiple innervation, and in g–i, NT = nerve terminal, TSC= terminal Schwann cell, M= muscle mitochondria, asterisks = secondary receptor folds, open star = engulfed axon material inside a Schwann cell.

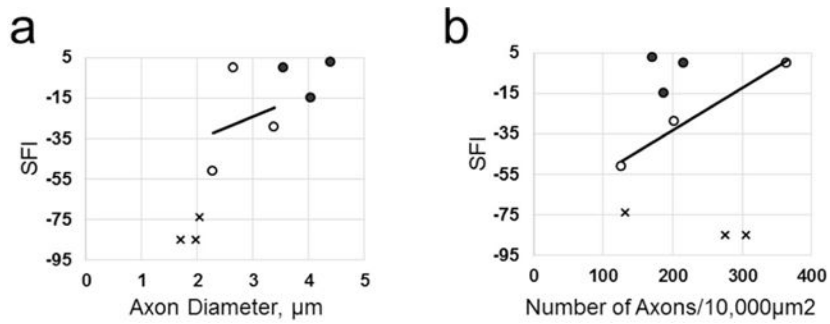

Figure 10.

Scatter plots of SFI scores assessing function/behavior and two morphological measures. Morphometric shown are axon diameter in µm (a) or axon density in # axons/10,000 µm2 (b) for Unoperated animals (filled circles), 42d PO PEG-fused (open circles), and 42d PO Negative Control animals (X points). Lines shown are best-fit linear regression lines through three data points for PEG-fused nerves. Note that PEG-fusion and Negative Control protocols are very different and independent procedures and the results for one are independent of (do not affect) the other.

Table 1

Primary antibodies used in this study.

Target/Antigen	Antibody	Antigen Species	Source	Immunogen	dilution	RRID
nerve terminals/Synaptic vesicle glycoprotein 2A	SV2-mouse monoclonal	Ommata (electric fish)	DSHB, cat# SV2	purified synaptic vesicles	1:400	AB_231 5385
neurofilament (NF-M)	2H3-mouse monoclonal	Rat	DSHB, cat#2H3	neonate rat brain cytoskeletal preparations	1:400	AB_531 793

Table 2

Nerve Fiber (MAX10): Average nerve fiber diameter (μm) and average diameter (μm) of the ten largest diameter fibers; MFA: muscle fiber cross-sectional area; MFI: percent of soleus muscle fibers having normal NMJs. Number of animals in data sample is given in the Avg axon diameter row when n>1. Not all parameters were measured for each individual animal, as indicated by blank cells. Yes, No: Muscle fiber innervation noted, but not counted. Table 2 gives the exact PO day that each animal was sampled, rather than giving a range of sampling day for which the same results would be expected, e.g., 7–14d PO.

Days PO	Animal, group	SFI	Avg axon diameter (μm)	Avg g ratio	Axons per 10,000μm^2 (density)	Nerve Fiber (MAX_{10})	MFA (μm^2)	MFI (%)
Unoperated								
	U2	3	4.40±1.96	0.62±0.06	171	7.0(11.9)		100%*
	U1	0	3.54±1.50	0.61±0.05	215	5.9(10.3)	2690±700	100%*
	U3	−15	3.49±1.16	0.61±0.06	187	5.7 (9.2)	2730±720	100%*
Unop Avg	**n=3**	**−4**	**3.82±1.64**	**0.61±0.06**	**191**	**6.2(11.9)**	**2710±710**	**100%**
7d PO								
	E55 PEG	−94	1.88±0.80	0.67±0.07	282	2.8 (5.2)		73%
	E54 PEG	−99	1.82±0.75	0.69±0.08	199	2.6 (5.0)		90%
7d PEG Avg	**n=2**	**−97**	**1.85±0.78**	**0.68±0.07**	**241**	**2.7 (5.5)**		**80%**
	E19 NC	−86	0	0	0	0		
	E27 NC	−97	0	0	0	0		
	E70 NC	−103						0%
7d NC Avg	**n=3**	**−95**	**0**	**0**	**0**	**0**		0%
10d PO								
	E48 PEG	−77	4.45±2.21	0.63±0.05	108	7.3 (16.6)		Yes
	E52 NC	−96	0	0	0	0		No
14d PO								
	E5 NC	−91	0	0	0	0		
	E15 NC	−97	0	0	0	0	1240±410	
	E17 NC	−115	0	0	0	0	1490±490	
14d NC Avg	**n=3**	**−101**	**0**	**0**	**0**	**0**	**1370±470**	
7-14d PO								
7-14d PEG Avg	**n=3**	**−90**	**2.69±1.86**	**0.66±0.07**	**196**	**4.2 (13.5)**		**80%**

Days PO	Animal, group	SFI	Avg axon diameter (μm)	Avg g ratio	Axons per 10,000μm^2 (density)	Nerve Fiber (MAX_{10})	MFA (μm^2)	MFI (%)
7-14d NC Avg	**n=7**	**−98**	**0**	**0**	**0**	**0**		**0%**
21d PO								
	E49 PEG	−49	4.25±2.19	0.65±0.06	61	6.4(13.1)		91%
	E53 PEG	−74	2.53±1.15	0.74±0.06	377	3.3 (6.9)		96%
	E50 PEG	−86	6.64±4.64	0.66±0.13	13	9.3(12.1)		26%
21 d PEG Avg	**n=3**	**−70**	**3.24±1.87**	**0.71±0.08**	**150**	**4.8 (14.8)**		**78%**
	E62 NC	−82	1.57±0.40	0.73±0.05	75	2.1 (3.2)		0%
	E63 NC	−91	1.93±0.42	0.79±0.04	156	2.4 (3.5)		0%
21 d NC Avg	**n=2**	**−87**	**1.72±0.44**	**0.76±0.05**	**116**	**2.3 (3.6)**		**0%**
42d PO								
	E32 PEG	0	2.65±1.19	0.69±0.08	364	3.7 (6.6)	1400±570	
	E33 PEG	−29	3.38±1.19	0.74±0.06	202	4.5 (7.3)	2400±620	
	E31 PEG	−51	2.28±1.12	0.66±0.08	126	3.4 (6.9)	1670±510	
	K13 PEG	−34						100%
42 PEG Avg	**n=4**	**−29**	**2.77±1.25**	**0.70±0.08**	**231**	**3.9 (7.6)**	**1780±710**	100%
	E36 NC	−74	2.04±0.91	0.66±0.08	132	3.0 (5.6)	1500±530	
	E37 NC	−85	1.96±0.80	0.63±0.08	275	3.0 (5.2)	1510±420	
	E7 NC	−85	1.70±0.72	0.64±0.09	305	2.6 (5.0)		
	E11 NC	−94					1300±520	
42d NC Avg	**n=4**	**−85**	**1.90±0.83**	**0.65±0.09**	**237**	**2.9 (5.7)**	**1440±500**	

Table 3

Comparisons between Unoperated, PEG, and Negative Control axons at 7, 21, and 42d PO based on Students T test and Cohen's size effect d of the magnitude of difference between means (See Methods).

Comparison			Axon Diameter			g ratio	
Single cut-distal			**T test**	**Size Effect**	**T test**		**Size Effect**
7-14d PEG	vs	**Unop**	p <0.001	***d* = 0.65**	p <0.001		***d* =0.75**
7-14d PEG	**vs**	**7-14d NC**	–	–	–		–
7-14d NC	**vs**	**Unop**	–	–	–		–
21d PEG	**vs**	**Unop**	p <0.001	***d* = 0.33**	p < 0.001		***d* = 1.36**
21d PEG	**vs**	**21d NC**	p < 0.001	***d* = 1.12**	p < 0.001		***d* = 0.76**
21d NC	**vs**	**Unop**	p <0.001	***d* = 1.75**	p < 0.001		***d* = 2.62**
42d PEG	**vs**	**Unop**	p <0.001	***d* = 0.72**	p <0.001		***d* = 1.25**
42d PEG	**vs**	**42d NC**	p <0.001	***d* = 0.82**	p < 0.001		***d* = 0.65**
42d NC	**vs**	**Unop**	p < 0.001	***d* = 1.48**	p < 0.001		***d* = 0.44**